



**University of
Zurich**^{UZH}

**Zurich Open Repository and
Archive**

University of Zurich
University Library
Strickhofstrasse 39
CH-8057 Zurich
www.zora.uzh.ch

Year: 2016

CP-even scalar boson production via gluon fusion at the LHC

Anastasiou, Charalampos ; Duhr, Claude ; Dulat, Falko ; Furlan, Elisabetta ; Gehrmann, Thomas ;
Herzog, Franz ; Lazopoulos, Achilleas ; Mistlberger, Bernhard

Abstract: In view of the searches at the LHC for scalar particle resonances in addition to the 125 GeV Higgs boson, we present the cross-section for a CP-even scalar produced via gluon fusion at N³LO in perturbative QCD assuming that it couples directly to gluons in an effective theory approach. We refine our prediction by taking into account the possibility that the scalar couples to the top-quark and computing the corresponding contributions through NLO in perturbative QCD. We assess the theoretical uncertainties of the crosssection due to missing higher-order QCD effects and we provide the necessary information for obtaining the cross-section value and uncertainty from our results in specific scenarios beyond the Standard Model. We also give detailed results for the case of a 750 GeV scalar, which will be the subject of intense experimental studies.

DOI: [https://doi.org/10.1007/JHEP09\(2016\)037](https://doi.org/10.1007/JHEP09(2016)037)

Posted at the Zurich Open Repository and Archive, University of Zurich

ZORA URL: <https://doi.org/10.5167/uzh-129834>

Journal Article

Published Version



The following work is licensed under a Creative Commons: Attribution 4.0 International (CC BY 4.0) License.

Originally published at:

Anastasiou, Charalampos; Duhr, Claude; Dulat, Falko; Furlan, Elisabetta; Gehrmann, Thomas; Herzog, Franz; Lazopoulos, Achilleas; Mistlberger, Bernhard (2016). CP-even scalar boson production via gluon fusion at the LHC. *Journal of High Energy Physics*, 2016(9):37.

DOI: [https://doi.org/10.1007/JHEP09\(2016\)037](https://doi.org/10.1007/JHEP09(2016)037)

CP-even scalar boson production via gluon fusion at the LHC

Charalampos Anastasiou,^a Claude Duhr,^{b,c,1} Falko Dulat,^a Elisabetta Furlan,^{a,d}
Thomas Gehrmann,^e Franz Herzog,^f Achilleas Lazopoulos^a and Bernhard Mistlberger^b

^a*Institute for Theoretical Physics, ETH Zürich,
Wolfgang-Pauli-strasse 27, Zurich, 8093 Switzerland*

^b*Theoretical Physics department, CERN,
Geneve 23, 1211 Switzerland*

^c*Center for Cosmology, Particle Physics and Phenomenology (CP3),
Université catholique de Louvain, Chemin du Cyclotron 2, Louvain-La-Neuve, 1348 Belgium*

^d*Kavli Institute for Theoretical Physics, University of California,
Kohn Hall, Santa Barbara, CA, 93106 U.S.A.*

^e*Physik-Institut, Universität Zürich,
Winterthurerstrasse 190, Zürich, 8057 Switzerland*

^f*Nikhef,
Science Park 105, Amsterdam, NL-1098 XG The Netherlands*

E-mail: babis@phys.ethz.ch, claudeduhr@cern.ch,
dulatf@slac.stanford.edu, efurlan@phys.ethz.ch,
thomas.gehrmann@uzh.ch, fherzog@nikhef.nl, lazopoli@phys.ethz.ch,
bernhard.mistlberger@cern.ch

ABSTRACT: In view of the searches at the LHC for scalar particle resonances in addition to the 125 GeV Higgs boson, we present the cross-section for a CP-even scalar produced via gluon fusion at N³LO in perturbative QCD assuming that it couples directly to gluons in an effective theory approach. We refine our prediction by taking into account the possibility that the scalar couples to the top-quark and computing the corresponding contributions through NLO in perturbative QCD. We assess the theoretical uncertainties of the cross-section due to missing higher-order QCD effects and we provide the necessary information for obtaining the cross-section value and uncertainty from our results in specific scenarios beyond the Standard Model. We also give detailed results for the case of a 750 GeV scalar, which will be the subject of intense experimental studies.

KEYWORDS: QCD Phenomenology

ARXIV EPRINT: [1605.05761](https://arxiv.org/abs/1605.05761)

¹On leave from the ‘Fonds National de la Recherche Scientifique’ (FNRS), Belgium.

Contents

1	Introduction	1
2	N³LO QCD corrections in the effective theory approach	2
3	Finite width effects and the line-shape	5
4	Validity of the EFT approach	8
5	Top-quark contributions	10
6	Conclusion	16
A	Reference tables for the production cross-section of a CP-even scalar through top-quark loops	17

1 Introduction

The Higgs boson is the only elementary scalar particle of the Standard Model (SM) and the first such particle whose existence has been confirmed experimentally [1, 2]. Many well-motivated extensions of the SM predict additional electrically neutral and colourless scalar particles (elementary or not). Experimental searches to hunt for these hypothetical new particles are thus of extreme importance. The LHC experiments have the potential to discover new scalar resonances by using similar techniques and signatures as in the search for the SM Higgs boson. In particular, in this context both the ATLAS and CMS experiments have recently reported an excess in the diphoton mass spectrum at an invariant mass of ~ 750 GeV [3, 4]. Even if it is still premature to speculate if the source of this excess is indeed a new resonance or merely a statistical fluctuation, this excess is exemplary for the kind of signals that may arise from the production of heavy singlet scalars in the current run of the LHC.

While specific models with colour-neutral scalars may differ drastically in the principles which motivate them as well as in their spectra and interactions, the computation of QCD radiative corrections to their production cross-section could share many common features that are independent of the underlying model. In particular, the production of hypothetical Higgs-like scalars at the LHC may be favourable in the gluon-fusion process due to the large value of the gluon-gluon luminosity. In this case, the model-dependence of the production cross-section may only enter through the coupling describing the (effective) interaction of the Higgs-like scalar with the gluons and quarks.

The purpose of this paper is to provide benchmark cross-sections for a colorless CP-even scalar in an effective theory which is similar to the one obtained for the Higgs boson

in the Standard Model after integrating out the top-quark. The cross-section for the scalar can be obtained from the cross-section of the Higgs boson for a wide range of models, by appropriately taking into account the corresponding Wilson coefficient. Our computation is valid through N³LO in perturbative QCD and is based on recent results for the SM Higgs boson gluon-fusion cross-section to that order [5–20]. We consider mass values for the new scalar particle ranging from 10 GeV to 3 TeV, which is the same range as the one targeted by the searches of ATLAS and CMS in the Run 2 of the LHC [21].

In some extensions of the Standard Model (see, for example, ref. [22] and references therein) the new Higgs-like scalar has a non-negligible coupling to the Standard Model top-quark. For scalar masses below the top-pair threshold the Wilson coefficient in our effective field theory (EFT) can be made to account for a coupling of the scalar to the top-quark. However, for scalar masses around and above threshold, the effective theory approach is not accurate. For this purpose, we extend the effective theory by adding a Yukawa-type interaction of the top-quark with the scalar and compute the additional contributions generated by this coupling.

While we can correct our N³LO cross-section in the effective theory for contributions of light Standard Model particles through NLO in QCD, it is not possible to do so in a model-independent way for contributions from new relatively light particles with a mass smaller than about half the mass of the scalar. The presence of such particles will invalidate our effective-theory computation. To estimate this effect, we consider the difference between the effective theory NLO cross-section and the exact NLO cross-section for a 750 GeV scalar which couples to a new top-like quark, as a function of the mass of the quark. We find that the two cross-sections can differ by more than the QCD scale uncertainty for top-like quark masses as heavy as twice the mass of the scalar. Nevertheless, we observe that one can still make use of the effective theory computation for such a model also for lower values of the quark mass in order to estimate the relative size of the QCD corrections (K -factor).

This article is organised as follows. In section 2 we present the effective theory setup of our calculation and discuss how the results can be adapted to suite a large class of models through the Wilson coefficient. We also discuss the theoretical uncertainty that is associated with the N³LO QCD corrections in the effective theory. In section 3, we discuss the inclusion of finite width effects in the calculation and provide a fit of the zero-width cross-section to enable the adaptation of our results to models where the scalar resonance is expected to have a non-vanishing but narrow width. In section 4, we investigate the validity of our effective theory approach under the assumption that the coupling between the scalar and the gluons is mediated by a heavy top partner of varying mass. In section 5 we go beyond a purely effective description of the scalar interaction and allow for a non-vanishing coupling between the Standard Model top and the scalar, for which we present the NLO QCD corrections. We conclude in section 6 and provide appendices with tables of cross-section values for a wide range of masses of the scalar.

2 N³LO QCD corrections in the effective theory approach

Let us consider a model where the SM is extended by a colourless singlet scalar S of mass m_S and width Γ_S , which only couples to the SM in a minimal way. For now, we assume

that the only SM fields that the new scalar S couples to are the gluons, through an effective operator of dimension five. We will discuss Yukawa couplings to heavy quarks in section 5. Such a model can be described by a Lagrangian of the form

$$\mathcal{L}_{\text{eff}} = \mathcal{L}_{\text{SM}} + \mathcal{L}_S - \frac{1}{4v} C_S S G_{\mu\nu}^a G_a^{\mu\nu}, \quad (2.1)$$

where \mathcal{L}_S collects the kinetic term and the potential of the scalar S . The vacuum expectation value v is [23],

$$v = \frac{1}{\sqrt{\sqrt{2}G_f}} = 246.22 \text{ GeV},$$

and C_S is a Wilson coefficient parametrizing the strength of the coupling of the particle S with the gluons. Except for the value of the Wilson coefficient, this is the same dimension-five operator as the one coupling the SM Higgs boson to the gluons, after the top-quark has been integrated out.

Since the scalar S couples to gluons, it can be produced at hadron colliders. Its hadronic production cross-section can be cast in the form

$$\sigma_S(m_S, \Gamma_S, \Lambda_{\text{UV}}) = |C_S(\mu, \Lambda_{\text{UV}})|^2 \eta(\mu, m_S, \Gamma_S), \quad (2.2)$$

where μ is the mass scale introduced by dimensional regularisation and Λ_{UV} is the scale of new physics, representing collectively the masses of the heavy particles in some ultraviolet (UV) completion of the theory. At all orders in perturbation theory, the cross-section is independent of the arbitrary scale μ , with the scale variation of the square of the Wilson coefficient cancelling the one of the matrix-elements η . Since η does not depend on Λ_{UV} , the scale dependence of the Wilson coefficient itself is universal, and it does not depend on the (renormalizable) UV completion of the effective theory. In particular, the renormalization group evolution equation that relates the Wilson coefficient at two different scales reads [24]:

$$\frac{C_S(\mu, \Lambda_{\text{UV}})}{C_S(\mu_0, \Lambda_{\text{UV}})} = \frac{\beta(\mu)}{\beta(\mu_0)} \frac{\alpha(\mu_0)}{\alpha(\mu)}, \quad (2.3)$$

with $\beta(\mu)$ the QCD β -function. We see that, as expected, the evolution equation only depends on the low-energy effective theory, and it is independent of the details of the UV completion. As a consequence, if we divide the production cross-section by the value of the Wilson coefficient at some reference scale μ_0 ,

$$\frac{\sigma_S(m_S, \Gamma_S, \Lambda_{\text{UV}})}{|C_S(\mu_0, \Lambda_{\text{UV}})|^2} = \left[\frac{\beta(\mu)}{\beta(\mu_0)} \frac{\alpha(\mu_0)}{\alpha(\mu)} \right]^2 \eta(\mu, m_S, \Gamma_S), \quad (2.4)$$

we obtain a universal ratio that does not depend on the UV completion (up to corrections due to differences that the various high-energy theories may induce on the width of the scalar particle S). In particular, since the dimension-five operator in eq. (2.1) is the same as the dimension-five operator mediating Higgs production in gluon fusion in the SM, we can extract the right-hand side of eq. (2.4) from Higgs production in gluon-fusion,

$$\sigma_S(m_S, \Gamma_S, \Lambda_{\text{UV}}) = \left| \frac{C_S(\mu_0, \Lambda_{\text{UV}})}{C(\mu_0, m_t)} \right|^2 \sigma_{\text{H}}(m_S, \Gamma_S, m_t). \quad (2.5)$$

Here σ_H is the gluon-fusion production cross-section of a Higgs boson of mass m_S and width Γ_S , in a variant of the SM with $N_f = 5$ massless quarks and the top-quark integrated out, m_t is the top-quark mass and $C(\mu_0, m_t)$ is the Wilson coefficient multiplying the SM gluon-fusion operator evaluated at our reference scale μ_0 . In the $\overline{\text{MS}}$ scheme it reads [25, 26]

$$\begin{aligned}
C(\mu, m_t) = & -\frac{a_s}{3} \left\{ 1 + a_s \frac{11}{4} + a_s^2 \left[\frac{2777}{288} - \frac{19}{16} \log \left(\frac{m_t^2}{\mu^2} \right) - N_f \left(\frac{67}{96} + \frac{1}{3} \log \left(\frac{m_t^2}{\mu^2} \right) \right) \right] \right. \\
& + a_s^3 \left[- \left(\frac{6865}{31104} + \frac{77}{1728} \log \left(\frac{m_t^2}{\mu^2} \right) + \frac{1}{18} \log^2 \left(\frac{m_t^2}{\mu^2} \right) \right) N_f^2 \right. \\
& + \left(\frac{23}{32} \log^2 \left(\frac{m_t^2}{\mu^2} \right) - \frac{55}{54} \log \left(\frac{m_t^2}{\mu^2} \right) + \frac{40291}{20736} - \frac{110779}{13824} \zeta_3 \right) N_f \\
& \left. \left. - \frac{2892659}{41472} + \frac{897943}{9216} \zeta_3 + \frac{209}{64} \log^2 \left(\frac{m_t^2}{\mu^2} \right) - \frac{1733}{288} \log \left(\frac{m_t^2}{\mu^2} \right) \right] + \mathcal{O}(a_s^4) \right\}, \tag{2.6}
\end{aligned}$$

with $a_s = \alpha_s(\mu)/\pi$, α_s being the strong coupling constant in QCD with $N_f = 5$ flavors. We note at this point that eq. (2.5) is valid to all orders in perturbation theory, and so neither σ_S nor σ_H depend on the arbitrary scales μ_0 and μ . They do, however, acquire a dependence on the scale μ once the perturbative series is truncated at some finite order. It is of course possible to further separate μ into a factorization and a renormalization scale, μ_f and μ_r , as it is customary, and we will assume in the following that this is done implicitly. In addition, σ_S also acquires a dependence on our reference scale μ_0 order by order in perturbation theory, resulting from the truncation of the perturbative expansion of the ratio of Wilson coefficients.

Equation (2.5) is the basic formula which allows us to predict the hadronic production cross-section of a generic CP-even singlet scalar through gluon-fusion to high order in perturbative QCD. Indeed, the gluon-fusion cross-section is known through N³LO in QCD in the large- m_t limit [19] (for $\Gamma_S = 0$) as an expansion around the Higgs threshold, and eq. (2.5) easily allows us to convert the result for the Higgs boson into the corresponding N³LO cross-section for a generic CP-even scalar.

At this point we need to make a small technical comment: both the ratio of Wilson coefficient and the Higgs production cross-section on the right-hand side of eq. (2.5) admit a perturbative expansion up to N³LO. Multiplying these two perturbative expansions, as suggested by eq. (2.5), introduces additional terms into the perturbative expansion which are of N⁴LO accuracy or higher, thus beyond the reach and the control of our N³LO computation. In ref. [19] it was shown that the numerical impact of these terms is captured by the scale variation at N³LO if the central scale is chosen as $\mu = m_S/2$, and the effects of such terms are therefore accounted for by the scale variation uncertainty assigned to our prediction.

A second comment regards the dependence of the Standard Model Wilson coefficient on the various scales. The SM Wilson coefficient $C(\mu_0, m_t)$ depends on the reference scale μ_0 and the top-quark mass m_t . While the value of μ_0 is arbitrary and can be chosen freely, in practise we choose the value of μ_0 to be the mass of the scalar, $\mu_0 = m_S$, and we set the value of the mass of the top quark to its physical value. In doing so, we may introduce

large logarithms into the computation, order by order in perturbation theory. For example, we see that at NNLO and N³LO the Wilson coefficient contains a logarithm of the form $\log(m_t/\mu_0)$. Similarly, the Wilson coefficient expression for the scalar $C_S(\mu_0, \Lambda_{UV})$ will contain logarithms of the type $\log(\Lambda_{UV}/\mu_0)$. In order to avoid large logarithms due to widely disparate scales in the ratio of the two Wilson coefficients, it may be preferable to evaluate the SM Wilson coefficient with a top-quark mass value $m_t \sim \Lambda_{UV}$ rather than its physical value. The value of the top mass entering the SM Higgs cross-section can easily be changed with a simple rescaling,

$$\sigma_H(m_S, \Gamma_S, \Lambda_{UV}) = \left| \frac{C(\mu_0, \Lambda_{UV})}{C(\mu_0, m_t)} \right|^2 \sigma_H(m_S, \Gamma_S, m_t). \quad (2.7)$$

Let us now discuss our predictions for the production cross-section σ_S . In figures 1–4 we show the effective theory cross-section $\sigma_H(m_S, \Gamma_S = 0, m_t)$ as a function of m_S through N³LO, at a proton-proton collider with a center-of-mass energy of 13 TeV. The theory uncertainty bands correspond to a variation of the scale $\mu = \mu_r = \mu_f$ in the range $\mu \in [m_S/4, m_S]$. The value of the top mass is set to $m_t(m_t) = 162.7$ GeV and we use the PDF4LHC15 [27] parton distribution function (PDF) set. We observe that for the range of scalar masses between 10 GeV and 3 TeV the N³LO scale variation band is always contained inside the NNLO band. This is also true for the lowest values of this mass range, $m_S \sim 10$ –50 GeV (figure 1), where one observes especially large corrections at NLO and NNLO. For higher masses, the scale variation is reduced. As an illustration, we show in figure 5 the scale dependence for the cross-section of a CP-even scalar with a mass of 750 GeV.

Sources of theoretical uncertainty affecting the gluon-fusion cross-section at N³LO other than scale variation have been considered in detail in ref. [19]. In particular, these sources of uncertainty are due to the lack of N³LO parton densities and to the truncation of the threshold expansion for the N³LO correction. In order to estimate the uncertainty on our computation, we follow faithfully the uncertainty estimation prescription of ref. [19] with one modification: the uncertainty due to the lack of N³LO parton densities is estimated here as the envelope of the corresponding uncertainties formed by using the CT14 [28], NNPDF30 [29] and PDF4LHC sets, which are themselves computed according to the prescription of ref. [19]. The reason for modifying the prescription in this case is that the PDF4LHC set leads to very small uncertainties for scalars in the region 500–1000 GeV and, in particular, to a vanishing uncertainty estimate for a scalar with mass around 770 GeV. This feature is not shared with individual PDF sets. We therefore use, conservatively, the envelope of CT14, NNPDF30 and PDF4LHC, which leads to an uncertainty due to the lack of N³LO parton densities at the level of 0.9%–3% for scalars in the range 50 GeV–TeV. This uncertainty remains of the order of a few percent also at lower masses, but it increases rapidly to $\mathcal{O}(10\%)$ for $m_S \lesssim 20$ GeV.

We present the cross-section values and uncertainties for this range of scalar masses in appendix A. In particular, in table 6 we focus on the range between 730 and 770 GeV.

3 Finite width effects and the line-shape

The results of the previous section hold formally only when the width of the scalar is set to zero. In many beyond the Standard Model (BSM) scenarios, however, finite-width effects

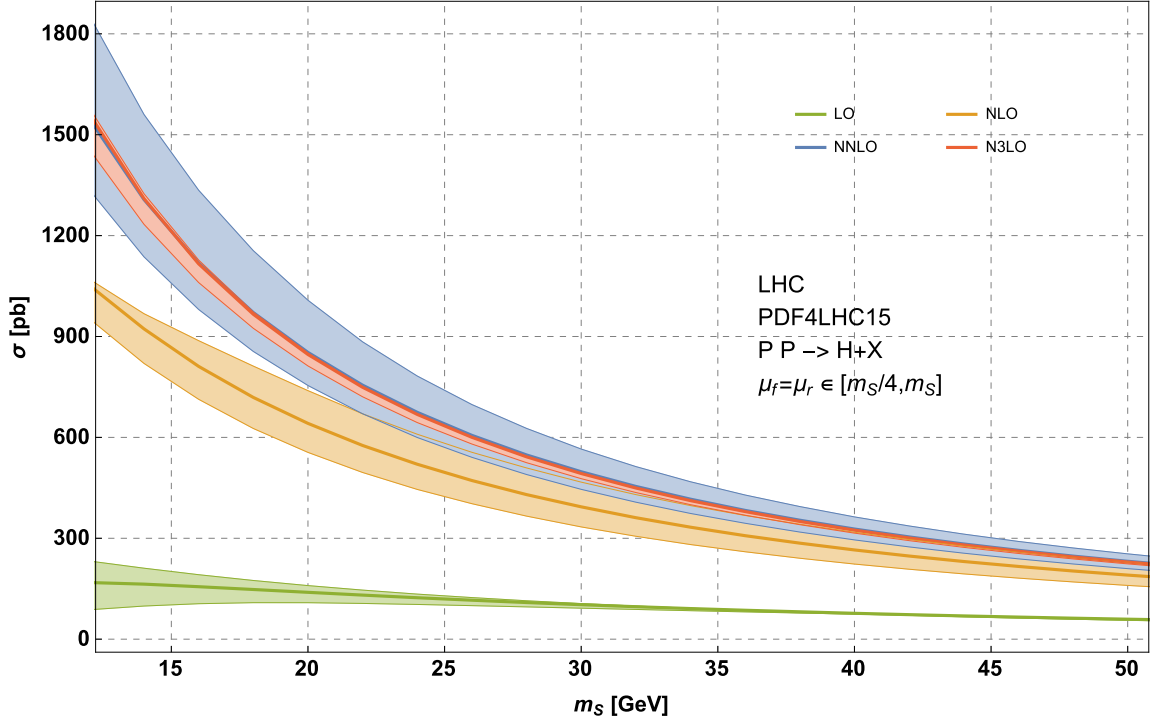


Figure 1. Effective theory production cross-section of a scalar particle as a function of the particle mass $m_S \in [10, 50]$ GeV through increasing orders in perturbation theory, at a 13 TeV proton-proton collider. The bands enveloping the respective orders represent the variation of the cross-section due to variations of the scale $\mu \in [m_S/4, m_S]$. The value of the top mass is set to $m_t(m_t) = 162.7$ GeV.

cannot be neglected. In this section we present a way to include leading finite-width effects into our results, in the case where the width is not too large compared to the mass.

The total cross-section for the production of a scalar boson of total width Γ_S can be obtained from the cross-section in the zero-width approximation via a convolution

$$\sigma_S(m_S, \Gamma_S, \Lambda_{UV}) = \int dQ^2 \frac{Q \Gamma_S(Q)}{\pi} \frac{\sigma_S(Q, \Gamma_S = 0, \Lambda_{UV})}{(Q^2 - m_S^2)^2 + m_S^2 \Gamma^2(m_S)} + \mathcal{O}(\Gamma_S(m_S)/m_S), \quad (3.1)$$

where Q is the virtuality of the scalar particle. This expression is accurate at leading order in $\Gamma_S(m_S)/m_S$. For large values of the width relative to the mass, subleading corrections and signal-background interference effects are important and are not captured by eq. (3.1). Let us also note that in order to use eq. (3.1) faithfully, one needs the width as a function of the virtuality of the scalar, which may bear a substantial model dependence. However, it is often the case that the width can be approximated as

$$\Gamma_S(Q \approx m_S) \equiv \Gamma_S. \quad (3.2)$$

The invariant mass distribution in this approximation for the production of a CP-even scalar with a mass of $m_S = 750$ GeV and total width from 2 to 10% of the scalar mass is shown in figure 6. This result has been obtained from an interpolation of the zero-width cross-section values of table 6 in appendix A. We caution that if the results of

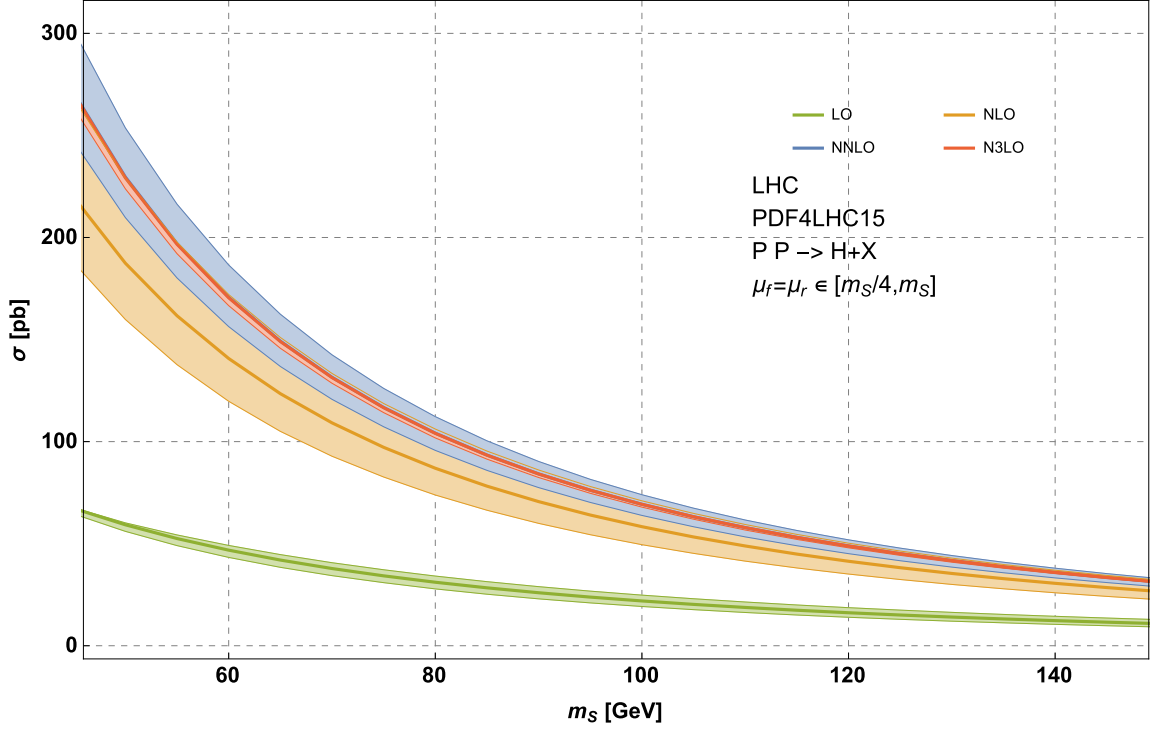


Figure 2. Effective theory production cross-section of a scalar particle of mass $m_S \in [50, 150]$ GeV through increasing orders in perturbation theory. For further details see the caption of figure 1.

appendix A are used to derive cross-section values with non-zero width effects following the strategy outlined in this section, an additional uncertainty of the order $\mathcal{O}(\Gamma_S/m_S)$ should be assigned.

In order to facilitate the computation of the line-shape we perform a parametric fit of the production cross-section of a zero-width scalar boson as a function of its virtuality (with $\Lambda_{UV} = m_S$) for a center-of-mass energy of 13 TeV. To guarantee agreement of the fitted cross-section with the actual cross-section at a level better than 1%, we split the range of interesting scalar boson mass values into three intervals:

- in the range $m_S \in [10 \text{ GeV}, 150 \text{ GeV}]$, cf. table 2 in appendix A, we find

$$\begin{aligned} \sigma_S(x) \approx & (3.89881 \times 10^6 x^2 - 1.90274 \times 10^6 x - 202261 x \log^2 x + 1623.77 \log^2 x \\ & - 923052 x \log x + 24108.2 \log x + 95652.2) \text{ pb}, \end{aligned} \quad (3.3)$$

- in the range $m_S \in [150 \text{ GeV}, 500 \text{ GeV}]$, cf. table 3, we find

$$\sigma_S(x) \approx (1 - \sqrt[3]{x})^{9.52798} x^{-0.0415044 \log x - 1.50381} \text{ pb}, \quad (3.4)$$

- in the range $m_S \in [500 \text{ GeV}, 3000 \text{ GeV}]$, cf. tables 4–5, we find

$$\sigma_S(x) \approx (1 - \sqrt[3]{x})^{9.71562} x^{-0.0040194 \log^3 x - 0.0474683 \log^2 x - 0.240878 \log x - 1.81243} \text{ pb}, \quad (3.5)$$

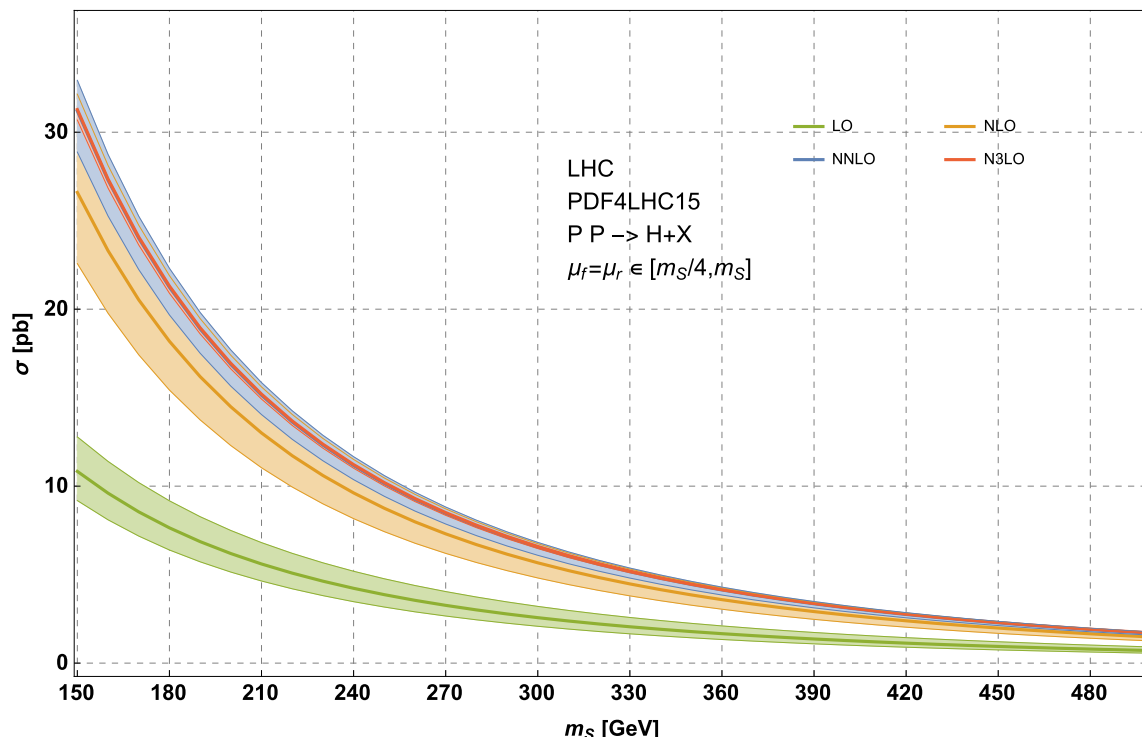


Figure 3. Effective theory production cross-section of a scalar particle with mass $m_S \in [150, 500]$ GeV through increasing orders in perturbation theory. For further details see the caption of figure 1.

where $x \equiv \frac{Q/\text{GeV}}{13\text{TeV}}$. The fits of eqs. (3.3)–(3.5) can be used as the kernel of the convolution in eq. (3.1).

4 Validity of the EFT approach

So far, we have assumed that the effective theory of eq. (2.1) furnishes an accurate description of the gluon-scalar interaction. However, this assumption may be challenged if the scalar couples to light coloured particles. To investigate this effect, we will consider a scalar of mass $m_S = 750\text{ GeV}$ which couples to a top-like quark of mass m_T . In this scenario, we can compute the cross-section exactly through NLO in perturbative QCD. We can then compare this prediction with the cross-section derived with the effective theory of eq. (2.1).

The red line in figure 7 shows the percent difference of the two predictions,

$$\delta_{\text{EFT}} = \frac{\sigma_{\text{exact}}^{\text{NLO}} - \sigma_{\text{EFT}}^{\text{NLO}}}{\sigma_{\text{exact}}^{\text{NLO}}} \times 100\%, \quad (4.1)$$

as a function of m_T for a scalar with a mass of $m_S = 750\text{ GeV}$. While in the region $m_T \sim m_S/2$ the effective field theory is inadequate, for larger values of m_T the EFT description becomes accurate very quickly. Indeed, for $m_T \sim 1.5m_S$ the discrepancy with

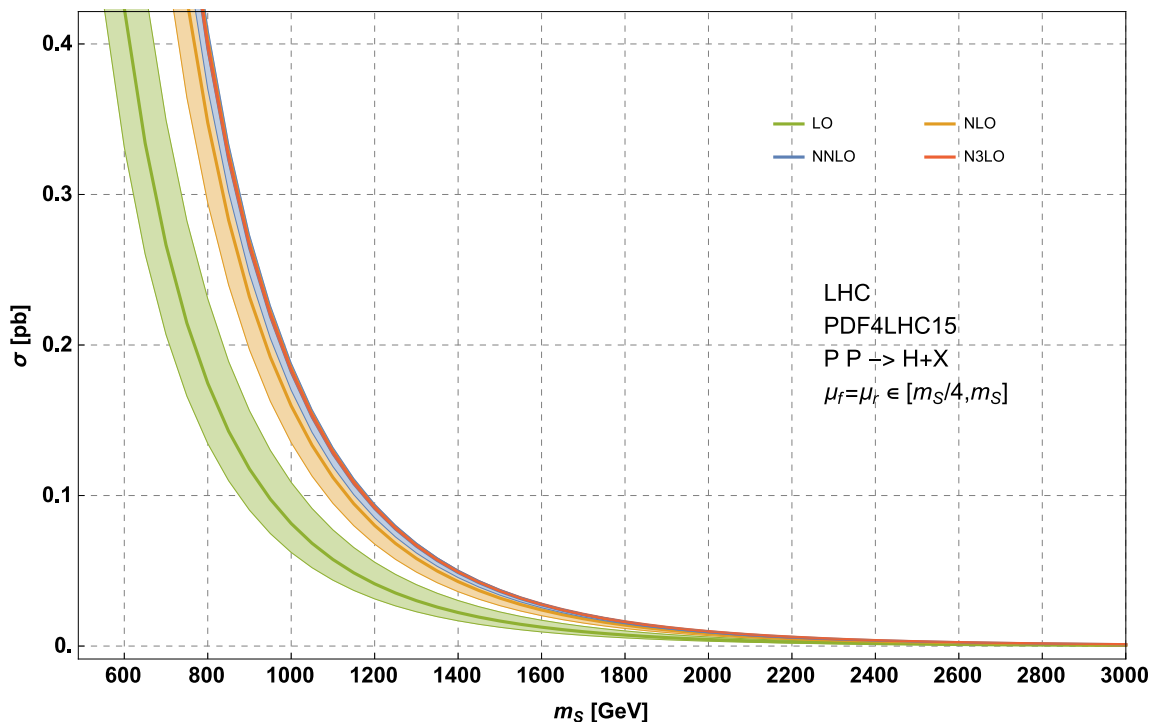


Figure 4. Effective theory production cross-section of a scalar particle as a function of the particle mass $m_S \in [500, 3000]$ GeV through increasing orders in perturbation theory. For further details see the caption of figure 1.

respect to the exact result is already below the theoretical uncertainty of QCD origin (of about 5%).

Let us now define a rescaled effective theory cross-section,

$$\sigma_{\text{rEFT}}^{\text{NLO}} = \frac{\sigma_{\text{exact}}^{\text{LO}}}{\sigma_{\text{EFT}}^{\text{LO}}} \sigma_{\text{EFT}}^{\text{NLO}}. \quad (4.2)$$

The green line of figure 7 shows the relative difference

$$\delta_{\text{rEFT}} = 100 \times \frac{\sigma_{\text{exact}}^{\text{NLO}} - \sigma_{\text{rEFT}}^{\text{NLO}}}{\sigma_{\text{exact}}^{\text{NLO}}} \quad (4.3)$$

between the rescaled effective theory prediction for the cross-section and the exact NLO cross-section. We notice that the rescaled effective theory cross-section reproduces the exact cross-section very well (as it has also been the case for the Standard Model Higgs boson [30, 31]).

We conclude that, while for the study of scalars which couple to relatively light particles one should resort to a calculation within a specific model, also in such situations the effective theory computation can be utilised as a means to compute with a good accuracy the corresponding QCD K -factor with respect to the exact LO cross-section.

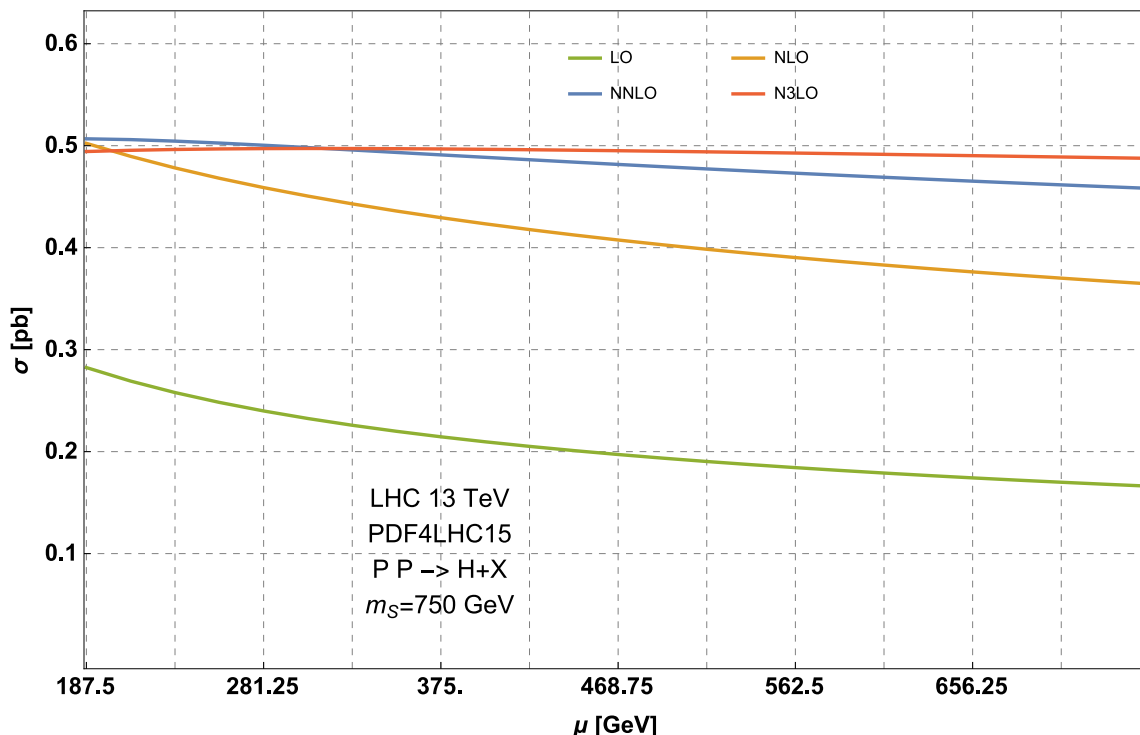


Figure 5. Effective theory production cross-section of a scalar particle with a mass $m_S = 750$ GeV as a function of the common renormalization and factorization scales μ through increasing orders in perturbation theory.

5 Top-quark contributions

So far we have considered the case where the interaction between the heavy scalar S and the Standard Model is mediated exclusively by the dimension-five operator in eq. (2.1). In many extensions of the Standard Model new scalars may also couple directly to the quarks of the third generation as well as the W and Z bosons. However, the absence of resonances in top-pair production and four-lepton production suggests that these couplings should be small. It may be nonetheless useful to estimate the contribution to the inclusive S -scalar cross-section due to the heavy SM quarks and gauge bosons for the purpose of setting precise experimental constraints on their couplings to S . In this section, we study the effects due to the top quark, which in many scenarios are expected to give the most important contribution.

For light scalar masses, $m_S < \mathcal{O}(m_t)$, contributions due to the coupling of the top quark can be simply taken into account through N³LO in perturbative QCD by using an appropriate Wilson coefficient C_S . For heavier scalars with masses around and above the top-pair threshold, however, it is not justified theoretically to integrate out the top-quark. For this reason we study in the following the effect of modifying the Lagrangian in eq. (2.1) by including a direct Yukawa interaction between the scalar S and the top quark, i.e., we consider the Lagrangian

$$\mathcal{L}_{\text{eff}} = \mathcal{L}_{\text{SM}} + \mathcal{L}_S - \frac{\lambda_{\text{wc}}}{4v} C S G_{\mu\nu}^a G_a^{\mu\nu} - \lambda_t \frac{m_t}{v} S \bar{t} t, \quad (5.1)$$

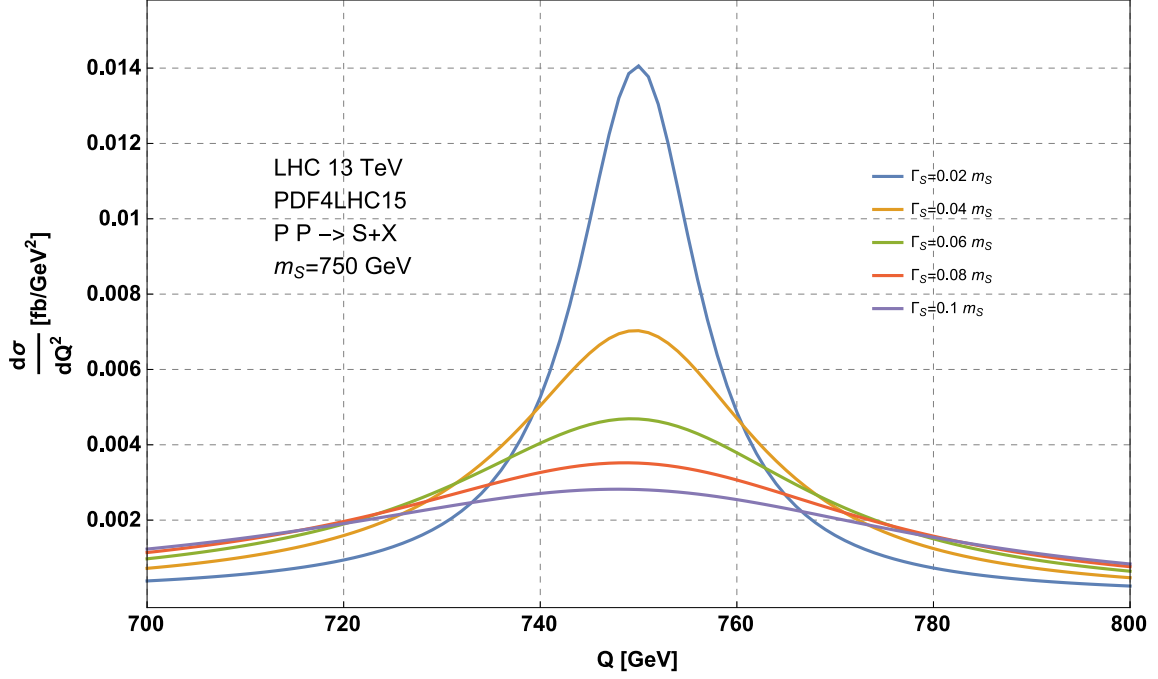


Figure 6. Line-shape of a 750 GeV CP-even scalar boson at the LHC for different values of its total width.

where λ_t is the ratio of the Yukawa coupling of the scalar S and the Yukawa coupling of the Higgs boson to the top quark and $\lambda_{wc} = \frac{C_S}{C}$ denotes the ratio of the Wilson coefficients in this theory and the SM with the top-quark integrated out.

The production cross-section now depends on the values of λ_{wc} and λ_t :

$$\sigma_S \equiv \sigma_S[\lambda_{wc}, \lambda_t]. \quad (5.2)$$

It does not take too much effort to show that the NLO cross-section can be cast in the form

$$\sigma_S^{\text{NLO}}[\lambda_{wc}, \lambda_t] = \lambda_{wc}(\lambda_{wc} - \lambda_t)\sigma_S^{\text{NLO}}[1, 0] + \lambda_t(\lambda_t - \lambda_{wc})\sigma_S^{\text{NLO}}[0, 1] + \lambda_{wc}\lambda_t\sigma_S^{\text{NLO}}[1, 1]. \quad (5.3)$$

The cross-section components of eq. (5.3) are shown in figure 8 as a function of the scalar mass. The cross-section with no Yukawa coupling, $\sigma_S^{\text{NLO}}[1, 0]$, is known through N³LO. Hence, we can improve the previous expression by including all N³LO corrections to the terms proportional to λ_{wc}^2 ,

$$\sigma_S[\lambda_{wc}, \lambda_t] = \lambda_{wc}^2\sigma_S^{\text{N}^3\text{LO}}[1, 0] - \lambda_{wc}\lambda_t\sigma_S^{\text{NLO}}[1, 0] + \lambda_t(\lambda_t - \lambda_{wc})\sigma_S^{\text{NLO}}[0, 1] + \lambda_{wc}\lambda_t\sigma_S^{\text{NLO}}[1, 1]. \quad (5.4)$$

Although we have taken into account QCD corrections within the EFT framework through N³LO, the result for the cross-section is formally only NLO-accurate because we are missing finite-mass effects beyond NLO. We therefore estimate the uncertainties on the NLO cross-section as

$$\frac{\delta\sigma^{\text{NLO}}[n_1, n_2]}{\sigma^{\text{NLO}}[n_1, n_2]} = \pm\delta_{>\text{NLO}}(1 + \delta_{\text{scheme}}[n_1, n_2]), \quad n_i \in \{0, 1\}, \quad (5.5)$$

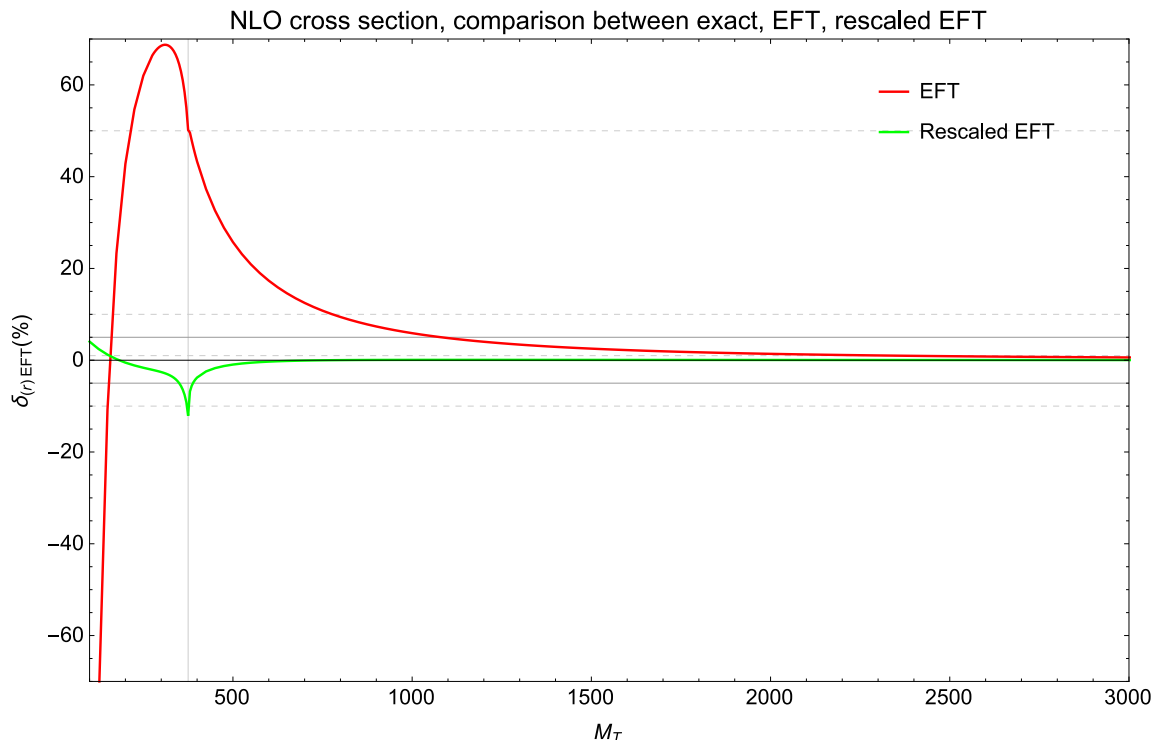


Figure 7. Percent difference (4.3) between the exact and rescaled EFT (rEFT) cross-section at NLO (red line/green line) as a function of the quark mass for the production of a 750 GeV CP-even scalar. The vertical line corresponds to $m_S/2$.

where

$$\delta_{>\text{NLO}} = \left(\frac{\sigma^{\text{N}^3\text{LO}}[1, 0] - \sigma^{\text{NLO}}[1, 0]}{\sigma^{\text{NLO}}[1, 0]} \right)_{\text{EFT}} \quad (5.6)$$

is the relative change of the gluon-fusion cross-section in the effective theory from NLO to N^3LO . Note that in this way make the assumption that the cross-section components that are not known beyond NLO will not have a worse perturbative convergence than in the effective theory. Finally, we enlarge this uncertainty further by

$$\delta_{\text{scheme}}[n_1, n_2] = \frac{\left| \sigma_{\text{exact}}^{\text{NLO}, \overline{\text{MS}}} [n_1, n_2] - \sigma_{\text{exact}}^{\text{NLO}, \text{OS}} [n_1, n_2] \right|}{\sigma_{\text{exact}}^{\text{NLO}, \overline{\text{MS}}} [n_1, n_2]}, \quad (5.7)$$

which measures the scheme dependence of the top-quark contribution at NLO.

Equation (5.4) is our best prediction for the gluon-fusion production cross-section of a generic scalar S . We recall that the values of $\sigma_S^{\text{N}^3\text{LO}}[1, 0]$ as a function of the scalar boson mass can be read off from tables 2–5 in appendix A. The NLO cross-sections $\sigma_S^{\text{NLO}}[n_1, n_2]$ ($n_1, n_2 \in \{0, 1\}$) are reported in tables 7–14. As an illustration, we present the complete set of terms entering in eq. (5.4) for a scalar of mass $m_S = 750$ GeV in table 1.

The following fits are a good approximation to the central values of the cross-sections introduced in this section. The fits are functions of $x = \frac{m_S/\text{GeV}}{13\text{TeV}}$ valid for a center-of-mass energy of 13 TeV and PDF4LHC15 parton distribution functions.

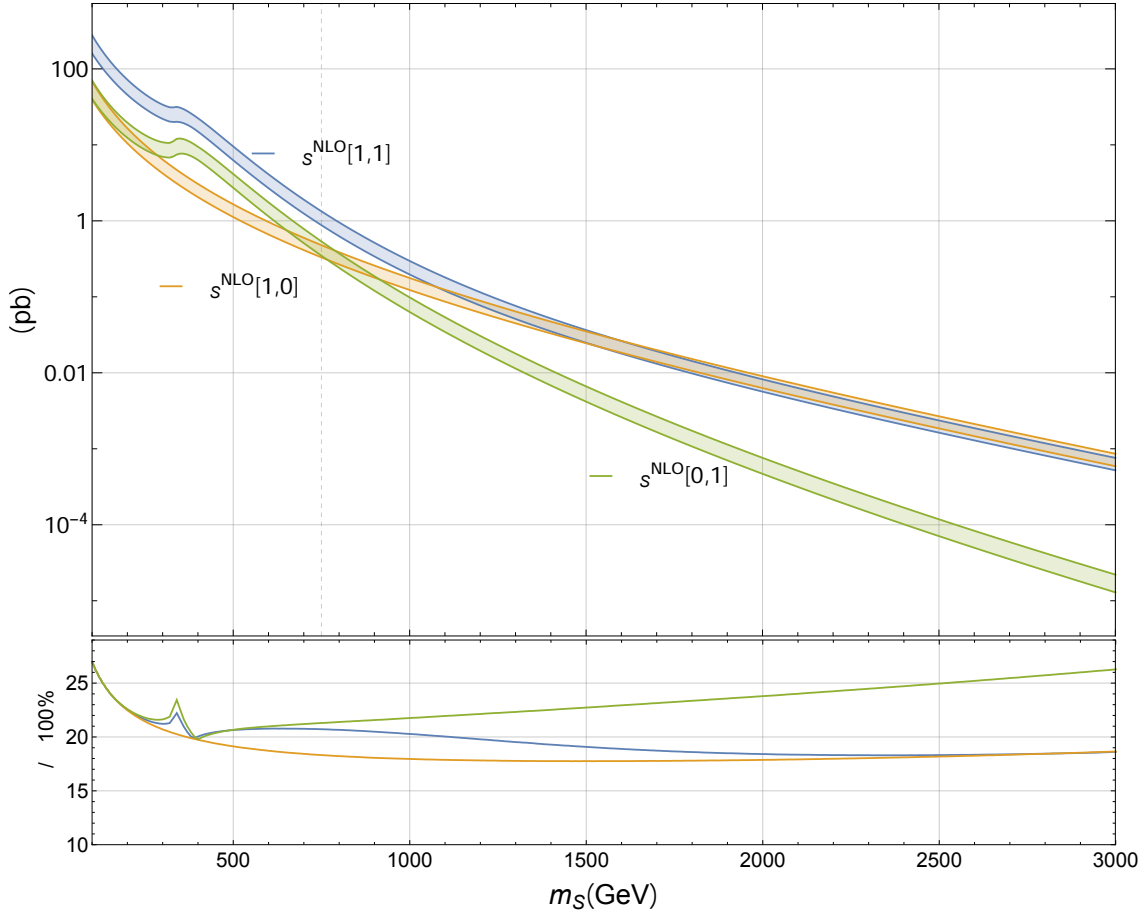


Figure 8. NLO contributions to the total cross-section for a scalar particle of mass m_S as described in eqs. (5.3), (5.4). The bands correspond to the theory uncertainty (based on eq. (5.5)). In the lower pane we present the relative theory uncertainty (%) for each of the contributions.

- In the range $m_S \in [50 \text{ GeV}, 150 \text{ GeV}]$, we find

$$\begin{aligned}
 \sigma_S^{\text{NLO}}[1,1]/\text{pb} = & -4.79097 \times 10^9 x^2 - \frac{454.08}{x^2} - \frac{48.2912 \log x}{x^2} + 1.4105 \times 10^9 x \\
 & - \frac{1.22684 \times 10^6}{x} + 1.79376 \times 10^7 \log^2 x + 1.11478 \times 10^9 x \log x \\
 & + 1.59613 \times 10^8 \log x - \frac{168047 \log x}{x} + 4.39955 \times 10^8,
 \end{aligned} \tag{5.8}$$

$$\begin{aligned}
 \sigma_S^{\text{NLO}}[1,0]/\text{pb} = & 2.71176 \times 10^9 x^2 + \frac{302.023}{x^2} + \frac{32.2322 \log x}{x^2} - 8.07812 \times 10^8 x \\
 & + \frac{787193}{x} - 1.11305 \times 10^7 \log^2 x - 6.62451 \times 10^8 x \log x \\
 & - 9.8134 \times 10^7 \log x + \frac{108365 \log x}{x} - 2.68924 \times 10^8,
 \end{aligned} \tag{5.9}$$

\sqrt{s}	Component	value[fb]	$\delta(\text{theory})$ [%]	$\delta(\text{pdf}+\alpha_S)$ [%]
7 TeV	$\sigma_S^{\text{N}^3\text{LO}}[1, 0]$	69.72	$^{+2.0}_{-4.2}$	7.0
	$\sigma_S^{\text{NLO}}[1, 0]$	55.59	19.52	6.95
	$\sigma_S^{\text{NLO}}[0, 1]$	61.71	22.69	6.94
	$\sigma_S^{\text{NLO}}[1, 1]$	152.6	22.1	6.92
8 TeV	$\sigma_S^{\text{N}^3\text{LO}}[1, 0]$	111.4	$^{+1.9}_{-4.0}$	6.1
	$\sigma_S^{\text{NLO}}[1, 0]$	89.37	19.18	6.23
	$\sigma_S^{\text{NLO}}[0, 1]$	98.92	22.3	6.22
	$\sigma_S^{\text{NLO}}[1, 1]$	245.3	21.71	6.2
13 TeV	$\sigma_S^{\text{N}^3\text{LO}}[1, 0]$	496.9	$^{+2.0}_{-3.7}$	4.0
	$\sigma_S^{\text{NLO}}[1, 0]$	404.6	18.3	4.5
	$\sigma_S^{\text{NLO}}[0, 1]$	442.7	21.3	4.4
	$\sigma_S^{\text{NLO}}[1, 1]$	1108	20.7	4.4
14 TeV	$\sigma_S^{\text{N}^3\text{LO}}[1, 0]$	609.7	$^{+1.9}_{-3.7}$	3.8
	$\sigma_S^{\text{NLO}}[1, 0]$	497.3	18.21	4.26
	$\sigma_S^{\text{NLO}}[0, 1]$	543.	21.14	4.2
	$\sigma_S^{\text{NLO}}[1, 1]$	1361	20.57	4.21

Table 1. Contributions to the cross-section (5.4) for the production of a CP-even scalar with mass 750 GeV at a proton-proton collider.

$$\begin{aligned}
 \sigma_S^{\text{NLO}}[0, 1]/\text{pb} = & 910970 - 3.05552 \times 10^7 x^2 + 7.62007 \times 10^6 x - \frac{544.886}{x} \\
 & + 26407.1 \log^2 x + 3.86595 \times 10^6 x \log x + 290640 \log x \\
 & - \frac{58.3182 \log x}{x}.
 \end{aligned} \tag{5.10}$$

- In the range $m_S \in [150 \text{ GeV}, 350 \text{ GeV}]$, we find

$$\begin{aligned}
 \sigma_S^{\text{NLO}}[1, 1]/\text{pb} = & 5.78391 \times 10^{11} x^3 - 6.04905 \times 10^{12} x^3 \log x - 3.97065 \times 10^{12} x^2 \\
 & - 1.60239 \times 10^{12} x^2 \log x - 2.28312 \times 10^{11} x - \frac{7.35167 \times 10^6}{x} \\
 & + 1.05353 \times 10^8 \log^2 x - 4.9669 \times 10^{10} x \log x \\
 & + 6.11874 \times 10^8 \log x - \frac{865250 \log x}{x} + 5.46682 \times 10^8,
 \end{aligned} \tag{5.11}$$

$$\begin{aligned}
 \sigma_S^{\text{NLO}}[1, 0]/\text{pb} = & -1.18403 \times 10^{10} x^3 + 8.55496 \times 10^{10} x^3 \log x + 5.7597 \times 10^{10} x^2 \\
 & + 2.3659 \times 10^{10} x^2 \log x + 3.48892 \times 10^9 x + \frac{121488.}{x} \\
 & - 1.66608 \times 10^6 \log^2 x + 7.67582 \times 10^8 x \log x \\
 & - 9.42982 \times 10^6 \log x + \frac{14369.3 \log x}{x} - 7.62306 \times 10^6,
 \end{aligned} \tag{5.12}$$

$$\begin{aligned}
 \sigma_S^{\text{NLO}}[0, 1]/\text{pb} = & 3.58507 \times 10^{11} x^3 - 3.67114 \times 10^{12} x^3 \log x - 2.41271 \times 10^{12} x^2 \\
 & - 9.74512 \times 10^{11} x^2 \log x - 1.3909 \times 10^{11} x - \frac{4.49756 \times 10^6}{x} \\
 & + 6.4297 \times 10^7 \log^2 x - 3.02763 \times 10^{10} x \log x \\
 & + 3.72922 \times 10^8 \log x - \frac{529486 \log x}{x} + 3.31551 \times 10^8.
 \end{aligned} \tag{5.13}$$

- In the range $m_S \in [350 \text{ GeV}, 500 \text{ GeV}]$, we find

$$\begin{aligned}
 \sigma_S^{\text{NLO}}[1, 1]/\text{pb} = & -1.55048 \times 10^{10} x^2 + \frac{20602.3}{x^2} + 4.12759 \times 10^{10} x^2 \log x \\
 & + 3.27683 \times 10^{10} x + \frac{3.90175 \times 10^6}{x} - 1.00487 \times 10^8 \log^2 x \\
 & - \frac{1.21312 \times 10^6 \log^2 x}{x} + 1.28157 \times 10^{10} x \log x \\
 & - 1.37351 \times 10^8 \log x - \frac{6.26022 \times 10^6 \log x}{x} + 8.75837 \times 10^8,
 \end{aligned} \tag{5.14}$$

$$\begin{aligned}
 \sigma_S^{\text{NLO}}[1, 0]/\text{pb} = & -1.74667 \times 10^9 x^2 + \frac{2345.03}{x^2} + 4.57918 \times 10^9 x^2 \log x \\
 & + 3.64833 \times 10^9 x + \frac{450670}{x} - 1.12934 \times 10^7 \log^2 x \\
 & - \frac{137023 \log^2 x}{x} + 1.43013 \times 10^9 x \log x - 1.53273 \times 10^7 \log x \\
 & - \frac{704422 \log x}{x} + 9.83324 \times 10^7,
 \end{aligned} \tag{5.15}$$

$$\begin{aligned}
 \sigma_S^{\text{NLO}}[0, 1]/\text{pb} = & 1.59986 \times 10^9 x^2 - \frac{2171.87}{x^2} - 4.2072 \times 10^9 x^2 \log x \\
 & - 3.34991 \times 10^9 x - \frac{417719}{x} + 1.03789 \times 10^7 \log^2 x \\
 & + \frac{126226 \log^2 x}{x} - 1.3131 \times 10^9 x \log x + 1.40646 \times 10^7 \log x \\
 & + \frac{647893 \log x}{x} - 9.03229 \times 10^7.
 \end{aligned} \tag{5.16}$$

- In the range $m_S \in [500 \text{ GeV}, 1000 \text{ GeV}]$, we find

$$\begin{aligned}
 \sigma_S^{\text{NLO}}[1, 1]/\text{pb} = & 1.0459 \times 10^8 x^2 + \frac{478.474}{x^2} - 7.72699 \times 10^7 x^2 \log x \\
 & - 8.14486 \times 10^7 x - \frac{2.50557 \times 10^6}{x} - 95661.5 \log^2 x \\
 & - \frac{71863.4 \log^2 x}{x} - 7.67177 \times 10^7 x \log x \\
 & - 1.27372 \times 10^7 \log x - \frac{802665 \log x}{x} - 3.08306 \times 10^7,
 \end{aligned} \tag{5.17}$$

$$\begin{aligned}
 \sigma_S^{\text{NLO}}[1, 0]/\text{pb} = & 1.76181 \times 10^7 x^2 + \frac{81.1265}{x^2} - 1.3039 \times 10^7 x^2 \log x \\
 & - 1.37328 \times 10^7 x - \frac{421944}{x} - 16421.7 \log^2 x \\
 & - \frac{12116.3 \log^2 x}{x} - 1.29224 \times 10^7 x \log x \\
 & - 2.14537 \times 10^6 \log x - \frac{135235 \log x}{x} - 5.19164 \times 10^6,
 \end{aligned} \tag{5.18}$$

$$\begin{aligned}
 \sigma_S^{\text{NLO}}[0, 1]/\text{pb} = & 2.43245 \times 10^7 x^2 + \frac{110.92}{x^2} - 1.78774 \times 10^7 x^2 \log x \\
 & - 1.88708 \times 10^7 x - \frac{585093}{x} - 22465.3 \log^2 x \\
 & - \frac{16766.8 \log^2 x}{x} - 1.78573 \times 10^7 x \log x \\
 & - 2.97483 \times 10^6 \log x - \frac{187382 \log x}{x} - 7.19613 \times 10^6.
 \end{aligned} \tag{5.19}$$

- In the range $m_S \in [1000 \text{ GeV}, 3000 \text{ GeV}]$, we find

$$\begin{aligned}
 \sigma_S^{\text{NLO}}[1, 1]/\text{fb} = & x^{-0.407849 \log^3 x - 0.841896 \log^2 x + 77.9612 x \log x + 14.6265 \log x + 49.7825} \\
 & \times (1 - \sqrt[3]{x})^{-1.74158},
 \end{aligned} \tag{5.20}$$

$$\begin{aligned}
 \sigma_S^{\text{NLO}}[1, 0]/\text{fb} = & x^{-0.0682707 \log^3 x - 0.812125 \log^2 x - 2.68171 x \log x - 3.91644 \log x - 10.0547} \\
 & \times (1 - \sqrt[3]{x})^{7.95188},
 \end{aligned} \tag{5.21}$$

$$\begin{aligned}
 \sigma_S^{\text{NLO}}[0, 1]/\text{fb} = & x^{-2.40603 x + 0.812624 \log^2 x + 18.7175 x \log x + 6.90869 \log x + 12.7991} \\
 & \times (1 - \sqrt[3]{x})^{8.05859}.
 \end{aligned} \tag{5.22}$$

6 Conclusion

In this paper we have presented the most precise predictions for the production of a CP-even scalar produced in gluon fusion at the LHC. We assume that the coupling of the scalar to the gluons can be described in an effective field theory approach. This enables us to provide precision QCD corrections at N³LO to the production cross-section at the LHC.

We find that for a scalar with a mass of 750 GeV the N³LO corrections yield a theoretical uncertainty of $\sim 2\%$ when we choose the central renormalization and factorization scales to be $m_S/2$ and follow the prescriptions layed out in ref. [19].

If we assume that the effective theory Wilson coefficient coupling of the CP-even scalar and the gluons is generated by a heavy top-partner, we can estimate the validity of the effective description as a function of the heavy fermion mass. We find that in the threshold region, when the mass of the top-partner is about half the mass of the scalar, the corrections can be as large as $\sim 60\%$. However, from direct searches the low mass ranges for top-partners are tightly constrained, so that at least for the discussion of a 750 GeV scalar this configuration is unlikely. For heavier fermion masses the effective theory description performs very well and is already accurate at $\sim 5\%$ when then fermion mass is about 1.5 times the scalar mass.

Additionally, we have considered the case that the new scalar couples directly to the SM top quark. In this case we need to take into account the top corrections to the cross-section, which are unfortunately only available through NLO in QCD, and they thus come with uncertainties of up to $\sim 20\%$. We incorporate the top corrections to the scalar production cross-section as a function of the Yukawa coupling of the top quark to the scalar, allowing for a model-dependent choice of the parameters.

In summary, we have provided the ingredients to endow predictions for the production of a CP-even scalar at the LHC with the most precise QCD corrections available. The only assumptions that have been made in the calculation are that the scalar couples to the gluons through an effective theory like operator. By determining the Wilson coefficient for the scalar coupling to the gluons as well as the Yukawa coupling to the top within a concrete model, it is now possible, using the numbers provided here, to easily incorporate QCD corrections through N³LO into the cross-section predictions for the LHC. While the results presented in this article concern strictly the production of a CP-even scalar, we can use the same techniques to compute the cross-section for resonance production of different CP/spin types which may be phenomenologically relevant (see, for example, ref. [32]). This will be the subject of future works.

Acknowledgments

CD, EF and TG are grateful to the KITP, Santa Barbara, for the hospitality during the final stages of this work. We are grateful to Riccardo Barbieri and Giuliano Panico for useful dicussions. This research was supported in part by the National Science Foundation under Grant No. NSF PHY11-25915, by the Swiss National Science Foundation (SNF) under contracts 200021-165772 and 200020-162487 and by the European Commission through the ERC grants “pertQCD”, “HEPGAME” (320651), “HICCUP”, “MathAm” and “MC@NNLO” (340983).

A Reference tables for the production cross-section of a CP-even scalar through top-quark loops

Here we report the values of the N³LO production cross-section $\sigma_H(m_S, \Gamma_S = 0, m_t)$ for a scalar of mass $m_S \in [10 \text{ GeV}, 3 \text{ TeV}]$ at the 13 TeV LHC, in an effective theory where the top

quark has been integrated out. The $\overline{\text{MS}}$ -mass of the top quark is chosen to be 162.7 GeV. We also show the two components that enter this result (cf. eq. (5.4), with $\sigma_S \rightarrow \sigma_H$, $\Lambda_{\text{UV}} \rightarrow m_t$, $C_S(\mu, \Lambda_{\text{UV}}) \rightarrow C(\mu_0, m_t)$), i.e. the squared SM Wilson coefficient $|C(\mu_0 = m_S/2, m_t)|^2$ and the matrix-element η . The theory error is computed from the variation of the common renormalization and factorization scale μ in the range $[m_S/4, m_S]$. To it we add linearly the uncertainty from missing N³LO PDFs, evaluated following the method of section 2, and from the truncation of the threshold expansion. We refer to ref. [19] for an explanation of how the latter is computed. We use the PDF set PDF4LHC14 [27] and derive the combined PDF+ α_s error following the indications of the PDF4LHC working group.

m_S [GeV]	$C^2(\mu_0^2) \times 10^{-5}$	σ [pb]	$\delta(\text{theory})$ [%]	$\delta(\alpha_S + \text{PDF})$ [%]
10	4.646	1899.6	$^{+17.8}_{-21.3}$	± 12.2
15	3.806	1202.7	$^{+11.6}_{-15.}$	± 6.7
20	3.348	845.8	$^{+8.8}_{-11.8}$	± 5.4
25	3.05	632.2	$^{+7.1}_{-10.}$	± 4.9
30	2.836	492.3	$^{+6.1}_{-8.8}$	± 4.6
35	2.673	394.9	$^{+5.5}_{-7.8}$	± 4.3
40	2.543	324.	$^{+4.8}_{-7.3}$	± 4.2
45	2.436	270.6	$^{+4.3}_{-6.7}$	$\pm 4.$
50	2.347	229.4	$^{+3.7}_{-6.}$	$\pm 4.$
55	2.27	196.8	$^{+3.5}_{-5.7}$	± 3.8
60	2.203	170.6	$^{+3.2}_{-5.4}$	± 3.7
65	2.144	149.2	$^{+3.1}_{-5.2}$	± 3.7
70	2.092	131.5	$^{+2.8}_{-4.9}$	± 3.6
75	2.045	116.6	$^{+2.6}_{-4.7}$	± 3.6
80	2.002	104.1	$^{+2.5}_{-4.7}$	± 3.5
85	1.964	93.4	$^{+2.4}_{-4.5}$	± 3.5
90	1.928	84.2	$^{+2.3}_{-4.3}$	± 3.4
95	1.896	76.3	$^{+2.2}_{-4.1}$	± 3.4
100	1.865	69.3	$^{+2.}_{-4.}$	± 3.4
105	1.837	63.2	$^{+2.}_{-3.9}$	± 3.3
110	1.811	57.9	$^{+1.9}_{-3.9}$	± 3.3
115	1.787	53.1	$^{+1.8}_{-3.8}$	± 3.3
120	1.764	48.9	$^{+1.8}_{-3.7}$	± 3.2
125	1.742	45.2	$^{+1.7}_{-3.7}$	± 3.2
130	1.722	41.8	$^{+1.7}_{-3.6}$	± 3.2
135	1.702	38.8	$^{+1.6}_{-3.5}$	± 3.2
140	1.684	36.	$^{+1.6}_{-3.5}$	± 3.2
145	1.667	33.5	$^{+1.5}_{-3.5}$	± 3.2
150	1.65	31.3	$^{+1.5}_{-3.4}$	± 3.1

Table 2. Production cross-section for a scalar particle with a mass in the range 10 GeV to 150 GeV.

m_S [GeV]	$C^2(\mu_0^2) \times 10^{-5}$	σ [pb]	$\delta(\text{theory})$ [%]	$\delta(\alpha_S + \text{PDF})$ [%]
150	1.65	31.29	$^{+1.5}_{-3.4}$	± 3.1
160	1.619	27.37	$^{+1.5}_{-3.3}$	± 3.1
170	1.591	24.09	$^{+1.4}_{-3.2}$	± 3.1
180	1.565	21.32	$^{+1.3}_{-3.2}$	± 3.1
190	1.542	18.96	$^{+1.3}_{-3.1}$	$\pm 3.$
200	1.519	16.94	$^{+1.3}_{-3.2}$	$\pm 3.$
210	1.499	15.2	$^{+1.4}_{-3.2}$	$\pm 3.$
220	1.48	13.69	$^{+1.4}_{-3.2}$	$\pm 3.$
230	1.461	12.37	$^{+1.4}_{-3.2}$	$\pm 3.$
240	1.445	11.22	$^{+1.4}_{-3.2}$	$\pm 3.$
250	1.428	10.2	$^{+1.4}_{-3.2}$	$\pm 3.$
260	1.413	9.3	$^{+1.4}_{-3.2}$	$\pm 3.$
270	1.399	8.51	$^{+1.4}_{-3.2}$	$\pm 3.$
280	1.385	7.8	$^{+1.4}_{-3.2}$	$\pm 3.$
290	1.372	7.16	$^{+1.5}_{-3.2}$	$\pm 3.$
300	1.36	6.59	$^{+1.5}_{-3.2}$	$\pm 3.$
310	1.348	6.08	$^{+1.5}_{-3.3}$	$\pm 3.$
320	1.337	5.62	$^{+1.5}_{-3.2}$	$\pm 3.$
330	1.326	5.2	$^{+1.5}_{-3.3}$	$\pm 3.$
340	1.316	4.82	$^{+1.5}_{-3.3}$	$\pm 3.$
350	1.306	4.48	$^{+1.5}_{-3.3}$	$\pm 3.$
360	1.297	4.16	$^{+1.5}_{-3.3}$	$\pm 3.$
370	1.287	3.88	$^{+1.6}_{-3.3}$	$\pm 3.$
380	1.279	3.62	$^{+1.6}_{-3.3}$	$\pm 3.$
390	1.27	3.38	$^{+1.6}_{-3.3}$	± 3.1
400	1.262	3.16	$^{+1.6}_{-3.3}$	± 3.1
410	1.254	2.96	$^{+1.6}_{-3.4}$	± 3.1
420	1.246	2.77	$^{+1.6}_{-3.4}$	± 3.1
430	1.239	2.6	$^{+1.6}_{-3.4}$	± 3.1
440	1.232	2.44	$^{+1.7}_{-3.4}$	± 3.1
450	1.225	2.3	$^{+1.6}_{-3.4}$	± 3.1
460	1.218	2.16	$^{+1.7}_{-3.4}$	± 3.2
470	1.211	2.03	$^{+1.7}_{-3.4}$	± 3.2
480	1.205	1.92	$^{+1.7}_{-3.4}$	± 3.2
490	1.199	1.81	$^{+1.7}_{-3.4}$	± 3.2
500	1.193	1.71	$^{+1.7}_{-3.5}$	± 3.3

Table 3. Production cross-section for a scalar particle with a mass in the range 150 GeV to 500 GeV.

m_S [GeV]	$C^2(\mu_0^2) \times 10^{-5}$	σ [fb]	$\delta(\text{theory})$ [%]	$\delta(\alpha_S + \text{PDF})$ [%]
500	1.193	1708.9	$^{+1.7}_{-3.5}$	± 3.3
550	1.165	1297.2	$^{+1.8}_{-3.5}$	± 3.4
600	1.141	1001.	$^{+1.8}_{-3.6}$	± 3.5
650	1.119	783.4	$^{+1.9}_{-3.6}$	± 3.7
700	1.099	620.6	$^{+1.9}_{-3.7}$	± 3.8
750	1.081	496.9	$^{+2.}_{-3.7}$	$\pm 4.$
800	1.065	401.5	$^{+2.}_{-3.8}$	± 4.2
850	1.05	327.1	$^{+2.1}_{-3.8}$	± 4.4
900	1.036	268.5	$^{+2.1}_{-3.8}$	± 4.6
950	1.023	221.9	$^{+2.2}_{-3.9}$	± 4.8
1000	1.011	184.5	$^{+2.2}_{-4.}$	$\pm 5.$
1050	1.	154.2	$^{+2.2}_{-4.}$	± 5.2
1100	0.989	129.5	$^{+2.3}_{-4.}$	± 5.4
1150	0.979	109.3	$^{+2.3}_{-4.1}$	± 5.6
1200	0.97	92.6	$^{+2.3}_{-4.1}$	± 5.9
1250	0.961	78.8	$^{+2.3}_{-4.1}$	± 6.1
1300	0.953	67.3	$^{+2.4}_{-4.2}$	± 6.3
1350	0.945	57.6	$^{+2.3}_{-4.2}$	± 6.6
1400	0.937	49.5	$^{+2.4}_{-4.2}$	± 6.8
1450	0.93	42.7	$^{+2.4}_{-4.2}$	$\pm 7.$
1500	0.923	36.9	$^{+2.4}_{-4.3}$	± 7.3
1550	0.917	31.9	$^{+2.5}_{-4.3}$	± 7.6
1600	0.91	27.7	$^{+2.5}_{-4.3}$	± 7.8
1650	0.904	24.1	$^{+2.5}_{-4.4}$	± 8.1
1700	0.898	21.	$^{+2.5}_{-4.5}$	± 8.5

Table 4. Production cross-section for a scalar particle with a mass in the range 500 GeV to 1700 GeV.

m_S [GeV]	$C^2(\mu_0^2) \times 10^{-5}$	σ [fb]	$\delta(\text{theory})$ [%]	$\delta(\alpha_S + \text{PDF})$ [%]
1750	0.893	18.38	$^{+3.2}_{-4.4}$	± 8.7
1800	0.887	16.09	$^{+2.5}_{-4.4}$	± 8.9
1850	0.882	14.11	$^{+2.6}_{-4.4}$	± 9.1
1900	0.877	12.39	$^{+2.5}_{-4.4}$	± 9.4
1950	0.872	10.9	$^{+2.6}_{-4.5}$	± 9.7
2000	0.868	9.6	$^{+2.6}_{-4.5}$	± 9.7
2050	0.863	8.47	$^{+2.5}_{-4.5}$	$\pm 10.$
2100	0.859	7.48	$^{+2.6}_{-4.5}$	± 10.5
2150	0.855	6.62	$^{+2.6}_{-4.5}$	± 10.8
2200	0.85	5.86	$^{+2.7}_{-4.6}$	± 11.2
2250	0.846	5.19	$^{+2.6}_{-4.6}$	± 11.8
2300	0.843	4.61	$^{+2.6}_{-4.5}$	$\pm 12.$
2350	0.839	4.09	$^{+2.6}_{-4.5}$	± 12.1
2400	0.835	3.64	$^{+2.6}_{-4.5}$	± 12.4
2450	0.832	3.24	$^{+2.5}_{-4.5}$	± 12.7
2500	0.828	2.89	$^{+2.6}_{-4.5}$	± 13.1
2550	0.825	2.57	$^{+2.5}_{-4.5}$	± 13.4
2600	0.821	2.3	$^{+2.5}_{-4.5}$	± 13.7
2650	0.818	2.05	$^{+2.6}_{-4.6}$	± 14.1
2700	0.815	1.83	$^{+2.7}_{-4.7}$	± 14.5
2750	0.812	1.64	$^{+2.8}_{-4.8}$	± 14.8
2800	0.809	1.46	$^{+2.9}_{-4.9}$	± 15.2
2850	0.806	1.31	$^{+3.}_{-5.}$	± 15.6
2900	0.803	1.17	$^{+3.1}_{-5.2}$	± 15.9
2950	0.8	1.05	$^{+3.2}_{-5.3}$	± 16.3
3000	0.798	0.94	$^{+3.4}_{-5.5}$	± 16.7

Table 5. Production cross-section for a scalar particle with a mass in the range 1750 GeV to 3000 GeV.

m_S [GeV]	$C^2(\mu_0^2) \times 10^{-5}$	σ [fb]	$\delta(\text{theory})$ [%]	$\delta(\alpha_S + \text{PDF})$ [%]
730	1.088	542.4	$^{+2.}_{-3.7}$	± 3.9
731	1.088	540.	$^{+2.}_{-3.7}$	± 3.9
732	1.087	537.7	$^{+2.}_{-3.7}$	± 3.9
733	1.087	535.3	$^{+2.}_{-3.7}$	$\pm 4.$
734	1.087	532.9	$^{+2.}_{-3.7}$	$\pm 4.$
735	1.086	530.6	$^{+2.}_{-3.7}$	$\pm 4.$
736	1.086	528.3	$^{+2.}_{-3.7}$	$\pm 4.$
737	1.086	525.9	$^{+2.}_{-3.7}$	$\pm 4.$
738	1.085	523.6	$^{+2.}_{-3.7}$	$\pm 4.$
739	1.085	521.3	$^{+2.}_{-3.7}$	$\pm 4.$
740	1.085	519.	$^{+2.}_{-3.7}$	$\pm 4.$
741	1.084	516.8	$^{+2.}_{-3.7}$	$\pm 4.$
742	1.084	514.5	$^{+2.}_{-3.7}$	$\pm 4.$
743	1.083	512.3	$^{+2.}_{-3.7}$	$\pm 4.$
744	1.083	510.	$^{+2.}_{-3.7}$	$\pm 4.$
745	1.083	507.8	$^{+2.}_{-3.7}$	$\pm 4.$
746	1.082	505.6	$^{+2.}_{-3.7}$	$\pm 4.$
747	1.082	503.4	$^{+2.}_{-3.7}$	$\pm 4.$
748	1.082	501.2	$^{+2.}_{-3.7}$	$\pm 4.$
749	1.081	499.	$^{+2.}_{-3.7}$	$\pm 4.$
750	1.081	496.9	$^{+2.}_{-3.7}$	$\pm 4.$
751	1.081	494.7	$^{+2.}_{-3.7}$	$\pm 4.$
752	1.08	492.6	$^{+2.}_{-3.7}$	$\pm 4.$
753	1.08	490.4	$^{+2.}_{-3.7}$	$\pm 4.$
754	1.08	488.3	$^{+2.}_{-3.7}$	$\pm 4.$
755	1.079	486.2	$^{+2.}_{-3.7}$	$\pm 4.$
756	1.079	484.1	$^{+2.}_{-3.7}$	$\pm 4.$
757	1.079	482.	$^{+2.}_{-3.7}$	$\pm 4.$
758	1.078	479.9	$^{+2.}_{-3.7}$	$\pm 4.$
759	1.078	477.8	$^{+2.}_{-3.7}$	$\pm 4.$
760	1.078	475.8	$^{+2.}_{-3.7}$	$\pm 4.$
761	1.077	473.7	$^{+2.}_{-3.7}$	$\pm 4.$
762	1.077	471.7	$^{+2.}_{-3.7}$	$\pm 4.$
763	1.077	469.7	$^{+2.}_{-3.7}$	$\pm 4.$
764	1.076	467.7	$^{+2.}_{-3.7}$	$\pm 4.$
765	1.076	465.7	$^{+2.}_{-3.7}$	$\pm 4.$
766	1.076	463.7	$^{+2.}_{-3.7}$	$\pm 4.$
767	1.075	461.7	$^{+2.}_{-3.7}$	$\pm 4.$
768	1.075	459.7	$^{+2.}_{-3.7}$	$\pm 4.$
769	1.075	457.7	$^{+2.}_{-3.7}$	$\pm 4.$
770	1.074	455.8	$^{+2.}_{-3.7}$	$\pm 4.$

Table 6. Production cross-section for a scalar particle with a mass in the range 730 GeV to 770 GeV.

m_S [GeV]	$\sigma_S^{\text{NLO}}[1,1][\text{pb}]$	$\delta_{\text{th}} [\%]$	$\delta_{\alpha_S}^{\text{PDF}} [\%]$	$\sigma_S^{\text{NLO}}[1,0][\text{pb}]$	$\delta_{\text{th}} [\%]$	$\delta_{\alpha_S}^{\text{PDF}} [\%]$	$\sigma_S^{\text{NLO}}[0,1][\text{pb}]$	$\delta_{\text{th}} [\%]$	$\delta_{\alpha_S}^{\text{PDF}} [\%]$
50	687.1	34.22	4.24	171.4	34.22	4.25	172.3	34.24	4.25
55	593.9	32.97	4.12	148.1	32.96	4.12	149.	32.98	4.12
60	518.3	31.93	4.02	129.	31.92	4.02	130.2	31.94	4.02
65	455.9	31.03	3.92	113.4	31.02	3.93	114.6	31.04	3.93
70	404.	30.23	3.84	100.4	30.22	3.84	101.7	30.25	3.85
75	360.2	29.55	3.77	89.42	29.54	3.76	90.8	29.57	3.77
80	323.1	28.91	3.71	80.07	28.9	3.71	81.56	28.93	3.71
85	291.3	28.35	3.65	72.06	28.34	3.65	73.63	28.37	3.65
90	263.8	27.84	3.6	65.15	27.83	3.6	66.8	27.86	3.6
95	239.9	27.38	3.55	59.15	27.37	3.55	60.85	27.4	3.55
100	219.	26.96	3.51	53.9	26.96	3.51	55.66	26.98	3.51
105	200.6	26.58	3.47	49.3	26.57	3.47	51.09	26.59	3.47
110	184.4	26.22	3.43	45.22	26.21	3.43	47.06	26.23	3.43
115	170.	25.88	3.4	41.59	25.87	3.4	43.49	25.89	3.4
120	157.2	25.57	3.37	38.35	25.56	3.37	40.3	25.57	3.37
125	145.7	25.28	3.34	35.45	25.27	3.34	37.45	25.29	3.34
130	135.4	25.01	3.31	32.86	25.01	3.32	34.89	25.02	3.31
135	126.1	24.76	3.29	30.51	24.75	3.29	32.59	24.76	3.29
140	117.7	24.51	3.28	28.41	24.51	3.28	30.51	24.52	3.27
145	110.1	24.29	3.25	26.49	24.29	3.25	28.62	24.29	3.25
150	103.1	24.07	3.23	24.74	24.07	3.23	26.91	24.07	3.23
160	91.08	23.7	3.2	21.69	23.7	3.21	23.92	23.71	3.2
170	80.94	23.36	3.17	19.12	23.34	3.18	21.42	23.38	3.17
180	72.39	23.06	3.15	16.96	23.03	3.15	19.32	23.09	3.15
190	65.1	22.78	3.13	15.11	22.74	3.13	17.53	22.83	3.13
200	58.86	22.54	3.12	13.52	22.48	3.12	16.	22.6	3.11
210	53.49	22.31	3.11	12.15	22.23	3.11	14.69	22.39	3.1
220	48.83	22.11	3.1	10.95	22.01	3.11	13.57	22.21	3.1
230	44.79	21.93	3.1	9.911	21.81	3.1	12.6	22.05	3.09
240	41.27	21.77	3.1	8.996	21.61	3.1	11.77	21.92	3.09
250	38.2	21.63	3.1	8.189	21.43	3.1	11.05	21.8	3.09
260	35.51	21.51	3.1	7.475	21.27	3.11	10.44	21.71	3.09
270	33.17	21.4	3.11	6.84	21.11	3.11	9.919	21.65	3.1
280	31.13	21.32	3.11	6.274	20.97	3.12	9.49	21.61	3.11
290	29.38	21.26	3.12	5.767	20.83	3.13	9.148	21.61	3.11
300	27.89	21.23	3.13	5.312	20.7	3.14	8.895	21.64	3.12
310	26.68	21.24	3.14	4.903	20.58	3.15	8.742	21.74	3.13
320	25.74	21.3	3.15	4.533	20.46	3.17	8.704	21.89	3.14
330	25.59	21.75	3.17	4.199	20.35	3.19	9.09	22.67	3.16
340	25.87	22.23	3.19	3.895	20.25	3.21	9.742	23.45	3.19
350	25.37	21.6	3.22	3.62	20.15	3.23	9.915	22.53	3.21
360	24.37	20.96	3.24	3.368	20.06	3.25	9.775	21.64	3.23
370	23.1	20.47	3.26	3.139	19.97	3.27	9.437	20.99	3.26
380	21.67	20.06	3.28	2.929	19.88	3.3	8.98	20.47	3.28
390	20.19	19.88	3.31	2.736	19.8	3.32	8.457	20.05	3.3

Table 7. NLO contributions to the production cross-section for a scalar particle, as they are defined in eq. (5.4). The theory uncertainty is computed as in eq. (5.5).

m_S [GeV]	$\sigma_S^{\text{NLO}}[1, 1][\text{pb}]$	$\delta_{\text{th}} [\%]$	$\delta_{\alpha_S}^{\text{PDF}} [\%]$	$\sigma_S^{\text{NLO}}[1, 0][\text{pb}]$	$\delta_{\text{th}} [\%]$	$\delta_{\alpha_S}^{\text{PDF}} [\%]$	$\sigma_S^{\text{NLO}}[0, 1][\text{pb}]$	$\delta_{\text{th}} [\%]$	$\delta_{\alpha_S}^{\text{PDF}} [\%]$
400	18.71	20.03	3.33	2.559	19.73	3.35	7.905	19.76	3.33
410	17.28	20.14	3.35	2.397	19.65	3.37	7.347	19.92	3.35
420	15.91	20.24	3.38	2.247	19.58	3.4	6.8	20.06	3.37
430	14.61	20.31	3.4	2.109	19.51	3.43	6.275	20.17	3.4
440	13.41	20.38	3.43	1.981	19.45	3.45	5.776	20.27	3.42
450	12.29	20.43	3.46	1.863	19.39	3.48	5.308	20.35	3.45
460	11.26	20.48	3.48	1.754	19.33	3.51	4.872	20.42	3.48
470	10.31	20.52	3.51	1.652	19.27	3.54	4.467	20.48	3.5
480	9.442	20.56	3.54	1.558	19.22	3.57	4.094	20.54	3.53
490	8.647	20.59	3.57	1.47	19.17	3.6	3.751	20.59	3.56
500	7.921	20.61	3.6	1.388	19.11	3.63	3.436	20.64	3.59
510	7.258	20.64	3.62	1.312	19.07	3.66	3.147	20.68	3.62
520	6.654	20.66	3.65	1.241	19.02	3.69	2.883	20.72	3.65
530	6.104	20.68	3.68	1.175	18.98	3.72	2.642	20.75	3.68
540	5.602	20.69	3.72	1.113	18.93	3.75	2.422	20.79	3.71
550	5.145	20.7	3.75	1.055	18.89	3.78	2.221	20.82	3.74
560	4.729	20.71	3.78	1.	18.85	3.82	2.037	20.85	3.77
570	4.349	20.73	3.81	0.9494	18.82	3.85	1.87	20.88	3.8
580	4.003	20.73	3.84	0.9016	18.78	3.88	1.717	20.9	3.83
590	3.687	20.74	3.87	0.8567	18.74	3.91	1.578	20.93	3.86
600	3.399	20.74	3.9	0.8145	18.7	3.95	1.451	20.95	3.9
610	3.136	20.75	3.94	0.7748	18.67	3.98	1.335	20.98	3.93
620	2.896	20.75	3.97	0.7374	18.64	4.01	1.228	21.	3.96
630	2.677	20.74	4.	0.7022	18.61	4.04	1.131	21.02	3.99
640	2.476	20.75	4.04	0.669	18.58	4.08	1.043	21.04	4.03
650	2.292	20.74	4.07	0.6377	18.54	4.11	0.9616	21.05	4.06
660	2.123	20.74	4.1	0.6082	18.52	4.14	0.8873	21.08	4.09
670	1.969	20.74	4.14	0.5803	18.49	4.18	0.8193	21.1	4.13
680	1.827	20.73	4.17	0.5539	18.47	4.21	0.757	21.12	4.16
690	1.697	20.73	4.2	0.5289	18.44	4.25	0.6998	21.14	4.19
700	1.577	20.72	4.24	0.5053	18.42	4.28	0.6474	21.16	4.23
710	1.467	20.72	4.27	0.483	18.39	4.31	0.5993	21.18	4.26
720	1.366	20.71	4.31	0.4618	18.37	4.35	0.5551	21.2	4.3
730	1.273	20.7	4.34	0.4417	18.35	4.38	0.5144	21.21	4.33
740	1.187	20.69	4.37	0.4227	18.32	4.42	0.477	21.23	4.36
750	1.108	20.68	4.41	0.4046	18.3	4.45	0.4427	21.25	4.4
760	1.035	20.67	4.44	0.3875	18.28	4.49	0.411	21.27	4.43
770	0.967	20.66	4.48	0.3712	18.26	4.52	0.3818	21.29	4.47
780	0.9045	20.65	4.51	0.3557	18.24	4.55	0.3549	21.31	4.5
790	0.8467	20.63	4.55	0.341	18.22	4.59	0.3301	21.32	4.54
800	0.7932	20.62	4.58	0.327	18.21	4.62	0.3071	21.34	4.57
810	0.7435	20.61	4.62	0.3137	18.19	4.66	0.286	21.36	4.61
820	0.6976	20.6	4.65	0.301	18.17	4.69	0.2664	21.38	4.64
830	0.6549	20.58	4.69	0.2889	18.16	4.74	0.2483	21.4	4.68
840	0.6152	20.57	4.72	0.2774	18.14	4.76	0.2316	21.42	4.71

Table 8. NLO contributions to the production cross-section for a scalar particle, as they are defined in eq. (5.4). The theory uncertainty is computed as in eq. (5.5).

m_S [GeV]	$\sigma_S^{\text{NLO}}[1, 1][\text{fb}]$	$\delta_{\text{th}} [\%]$	$\delta_{\alpha_S}^{\text{PDF}} [\%]$	$\sigma_S^{\text{NLO}}[1, 0][\text{fb}]$	$\delta_{\text{th}} [\%]$	$\delta_{\alpha_S}^{\text{PDF}} [\%]$	$\sigma_S^{\text{NLO}}[0, 1][\text{fb}]$	$\delta_{\text{th}} [\%]$	$\delta_{\alpha_S}^{\text{PDF}} [\%]$
850	578.4	20.55	4.76	266.4	18.12	4.8	216.1	21.43	4.75
860	544.1	20.53	4.79	256.	18.11	4.83	201.7	21.45	4.79
870	512.2	20.51	4.83	246.	18.09	4.87	188.4	21.47	4.82
880	482.5	20.49	4.87	236.4	18.08	4.91	176.1	21.48	4.86
890	454.8	20.47	4.9	227.3	18.06	4.94	164.6	21.5	4.89
900	429.	20.45	4.94	218.7	18.05	4.98	154.	21.52	4.93
910	404.9	20.44	4.97	210.4	18.04	5.01	144.1	21.54	4.97
920	382.4	20.41	5.01	202.4	18.02	5.05	134.9	21.55	5.
930	361.4	20.4	5.04	194.8	18.01	5.08	126.4	21.57	5.04
940	341.7	20.38	5.08	187.6	18.	5.12	118.4	21.59	5.07
950	323.3	20.36	5.14	180.6	17.99	5.15	111.	21.61	5.11
960	306.1	20.33	5.19	174.	17.98	5.19	104.1	21.63	5.15
970	290.	20.31	5.22	167.6	17.97	5.23	97.73	21.65	5.18
980	274.8	20.29	5.25	161.5	17.96	5.26	91.74	21.66	5.22
990	260.6	20.27	5.26	155.7	17.95	5.3	86.16	21.68	5.26
1000	247.3	20.25	5.3	150.1	17.94	5.33	80.95	21.7	5.29
1010	234.8	20.23	5.33	144.8	17.93	5.37	76.09	21.72	5.33
1020	223.	20.2	5.37	139.6	17.92	5.41	71.55	21.74	5.37
1030	212.	20.18	5.41	134.7	17.91	5.44	67.3	21.76	5.4
1040	201.6	20.15	5.44	130.	17.91	5.48	63.34	21.78	5.44
1050	191.8	20.13	5.48	125.4	17.9	5.52	59.63	21.8	5.48
1060	182.5	20.11	5.52	121.1	17.89	5.55	56.15	21.82	5.51
1070	173.8	20.08	5.55	116.9	17.88	5.59	52.9	21.83	5.55
1080	165.6	20.06	5.59	112.9	17.87	5.63	49.86	21.85	5.59
1090	157.9	20.03	5.63	109.	17.87	5.66	47.	21.87	5.63
1100	150.6	20.01	5.66	105.3	17.86	5.7	44.33	21.89	5.66
1110	143.7	19.98	5.7	101.8	17.85	5.74	41.82	21.91	5.7
1120	137.2	19.96	5.74	98.33	17.85	5.77	39.47	21.93	5.74
1130	131.	19.93	5.77	95.04	17.84	5.81	37.27	21.94	5.78
1140	125.2	19.9	5.81	91.87	17.83	5.85	35.19	21.96	5.81
1150	119.6	19.88	5.85	88.83	17.83	5.88	33.25	21.98	5.85
1160	114.4	19.85	5.88	85.9	17.82	5.92	31.42	22.	5.89
1170	109.4	19.83	5.92	83.08	17.82	5.96	29.7	22.02	5.93
1180	104.7	19.8	5.96	80.36	17.81	6.	28.09	22.04	5.97
1190	100.3	19.78	6.	77.75	17.81	6.03	26.57	22.06	6.
1200	96.05	19.75	6.03	75.23	17.8	6.07	25.14	22.07	6.04
1210	92.03	19.73	6.07	72.81	17.8	6.11	23.8	22.1	6.08
1220	88.22	19.7	6.11	70.47	17.8	6.15	22.53	22.12	6.12
1230	84.59	19.68	6.15	68.22	17.79	6.18	21.34	22.13	6.16
1240	81.15	19.65	6.19	66.05	17.79	6.22	20.21	22.15	6.2
1250	77.87	19.63	6.22	63.96	17.78	6.26	19.15	22.17	6.24
1260	74.75	19.6	6.26	61.94	17.78	6.3	18.16	22.19	6.27
1270	71.78	19.57	6.3	60.	17.77	6.34	17.21	22.2	6.31
1280	68.96	19.55	6.34	58.12	17.77	6.37	16.33	22.23	6.35
1290	66.26	19.52	6.38	56.31	17.76	6.41	15.49	22.24	6.39

Table 9. NLO contributions to the production cross-section for a scalar particle, as they are defined in eq. (5.4). The theory uncertainty is computed as in eq. (5.5).

m_S [GeV]	$\sigma_S^{\text{NLO}}[1,1][\text{fb}]$	$\delta_{\text{th}} [\%]$	$\delta_{\alpha_S}^{\text{PDF}} [\%]$	$\sigma_S^{\text{NLO}}[1,0][\text{fb}]$	$\delta_{\text{th}} [\%]$	$\delta_{\alpha_S}^{\text{PDF}} [\%]$	$\sigma_S^{\text{NLO}}[0,1][\text{fb}]$	$\delta_{\text{th}} [\%]$	$\delta_{\alpha_S}^{\text{PDF}} [\%]$
1300	63.7	19.49	6.41	54.57	17.76	6.45	14.7	22.26	6.43
1310	61.23	19.48	6.46	52.88	17.76	6.49	13.95	22.28	6.47
1320	58.89	19.45	6.5	51.26	17.76	6.53	13.24	22.3	6.51
1330	56.65	19.44	6.54	49.69	17.75	6.57	12.58	22.32	6.55
1340	54.52	19.41	6.57	48.17	17.75	6.61	11.95	22.34	6.59
1350	52.5	19.39	6.6	46.71	17.75	6.64	11.35	22.36	6.63
1360	50.59	19.35	6.62	45.3	17.75	6.68	10.79	22.38	6.67
1370	48.73	19.33	6.67	43.93	17.74	6.72	10.25	22.4	6.71
1380	46.96	19.31	6.72	42.61	17.74	6.76	9.749	22.42	6.75
1390	45.26	19.28	6.76	41.33	17.74	6.8	9.272	22.43	6.79
1400	43.64	19.26	6.8	40.1	17.74	6.84	8.82	22.46	6.83
1410	42.09	19.24	6.84	38.91	17.74	6.88	8.392	22.48	6.87
1420	40.6	19.22	6.9	37.76	17.74	6.92	7.986	22.5	6.91
1430	39.17	19.2	6.95	36.65	17.74	6.96	7.602	22.52	6.95
1440	37.81	19.17	6.99	35.57	17.74	7.	7.238	22.54	6.99
1450	36.5	19.16	7.03	34.53	17.74	7.04	6.893	22.57	7.03
1460	35.24	19.13	7.06	33.52	17.74	7.08	6.566	22.58	7.07
1470	34.04	19.11	7.08	32.55	17.74	7.12	6.256	22.6	7.11
1480	32.89	19.09	7.12	31.6	17.74	7.16	5.961	22.62	7.15
1490	31.78	19.07	7.16	30.69	17.74	7.2	5.682	22.64	7.19
1500	30.72	19.05	7.2	29.81	17.74	7.24	5.417	22.66	7.23
1510	29.69	19.03	7.24	28.95	17.74	7.28	5.165	22.68	7.28
1520	28.71	19.01	7.28	28.12	17.74	7.32	4.926	22.7	7.32
1530	27.77	18.99	7.32	27.32	17.74	7.36	4.699	22.72	7.36
1540	26.86	18.97	7.36	26.55	17.74	7.4	4.483	22.74	7.4
1550	25.99	18.96	7.4	25.8	17.74	7.44	4.278	22.76	7.44
1560	25.15	18.94	7.44	25.07	17.74	7.48	4.083	22.78	7.48
1570	24.35	18.92	7.48	24.36	17.74	7.52	3.898	22.8	7.53
1580	23.57	18.9	7.52	23.68	17.74	7.56	3.722	22.82	7.57
1590	22.83	18.88	7.56	23.02	17.74	7.61	3.555	22.85	7.61
1600	22.11	18.87	7.6	22.38	17.74	7.65	3.395	22.87	7.65
1610	21.42	18.85	7.65	21.75	17.74	7.69	3.244	22.89	7.7
1620	20.75	18.83	7.69	21.15	17.74	7.73	3.099	22.9	7.74
1630	20.11	18.81	7.73	20.57	17.75	7.77	2.962	22.93	7.78
1640	19.49	18.8	7.77	20.	17.75	7.81	2.831	22.95	7.82
1650	18.89	18.78	7.81	19.45	17.75	7.86	2.707	22.97	7.87
1660	18.31	18.77	7.86	18.92	17.75	7.9	2.588	22.99	7.91
1670	17.76	18.75	7.9	18.4	17.75	7.94	2.475	23.01	7.95
1680	17.22	18.74	7.94	17.9	17.76	7.98	2.367	23.03	8.
1690	16.71	18.72	7.98	17.41	17.76	8.03	2.265	23.05	8.04
1700	16.21	18.7	8.02	16.94	17.75	8.07	2.167	23.07	8.08
1710	15.73	18.69	8.07	16.48	17.76	8.11	2.074	23.09	8.13
1720	15.26	18.68	8.11	16.04	17.76	8.16	1.985	23.11	8.17
1730	14.81	18.66	8.15	15.61	17.76	8.2	1.9	23.13	8.22
1740	14.38	18.65	8.2	15.19	17.76	8.24	1.819	23.15	8.26

Table 10. NLO contributions to the production cross-section for a scalar particle, as they are defined in eq. (5.4). The theory uncertainty is computed as in eq. (5.5).

m_S [GeV]	$\sigma_S^{\text{NLO}}[1, 1][\text{fb}]$	$\delta_{\text{th}} [\%]$	$\delta_{\alpha_S}^{\text{PDF}} [\%]$	$\sigma_S^{\text{NLO}}[1, 0][\text{fb}]$	$\delta_{\text{th}} [\%]$	$\delta_{\alpha_S}^{\text{PDF}} [\%]$	$\sigma_S^{\text{NLO}}[0, 1][\text{fb}]$	$\delta_{\text{th}} [\%]$	$\delta_{\alpha_S}^{\text{PDF}} [\%]$
1750	13.96	18.64	8.24	14.79	17.77	8.29	1.742	23.18	8.31
1760	13.56	18.63	8.28	14.39	17.77	8.33	1.668	23.2	8.35
1770	13.17	18.61	8.33	14.01	17.77	8.37	1.598	23.22	8.39
1780	12.79	18.6	8.37	13.64	17.78	8.42	1.531	23.24	8.44
1790	12.42	18.59	8.41	13.28	17.78	8.46	1.467	23.26	8.48
1800	12.07	18.57	8.46	12.93	17.78	8.5	1.405	23.28	8.53
1810	11.73	18.56	8.5	12.59	17.78	8.55	1.347	23.3	8.57
1820	11.4	18.55	8.54	12.26	17.79	8.59	1.291	23.32	8.62
1830	11.08	18.54	8.59	11.94	17.79	8.64	1.238	23.34	8.66
1840	10.77	18.53	8.63	11.62	17.79	8.68	1.187	23.36	8.71
1850	10.47	18.52	8.68	11.32	17.8	8.73	1.138	23.39	8.76
1860	10.18	18.51	8.72	11.03	17.8	8.77	1.092	23.41	8.8
1870	9.894	18.5	8.77	10.74	17.8	8.82	1.047	23.43	8.85
1880	9.621	18.49	8.81	10.46	17.8	8.86	1.004	23.45	8.89
1890	9.358	18.48	8.86	10.19	17.81	8.91	0.9637	23.47	8.94
1900	9.102	18.47	8.9	9.93	17.81	8.95	0.9248	23.49	8.99
1910	8.854	18.46	8.95	9.675	17.82	9.	0.8875	23.52	9.03
1920	8.614	18.45	8.99	9.427	17.82	9.04	0.8519	23.54	9.08
1930	8.382	18.44	9.04	9.186	17.82	9.09	0.8178	23.56	9.13
1940	8.156	18.44	9.08	8.951	17.83	9.14	0.7851	23.58	9.17
1950	7.937	18.43	9.13	8.723	17.83	9.18	0.7539	23.6	9.22
1960	7.725	18.42	9.18	8.502	17.83	9.23	0.724	23.62	9.27
1970	7.52	18.41	9.22	8.286	17.84	9.27	0.6953	23.64	9.32
1980	7.32	18.4	9.27	8.076	17.84	9.32	0.6679	23.67	9.37
1990	7.127	18.4	9.32	7.872	17.85	9.37	0.6416	23.69	9.41
2000	6.939	18.39	9.36	7.674	17.85	9.42	0.6164	23.71	9.46
2010	6.757	18.38	9.41	7.481	17.86	9.46	0.5923	23.73	9.51
2020	6.58	18.38	9.46	7.293	17.86	9.51	0.5692	23.75	9.56
2030	6.408	18.37	9.5	7.111	17.86	9.56	0.5471	23.77	9.61
2040	6.241	18.36	9.55	6.933	17.87	9.6	0.5259	23.79	9.65
2050	6.08	18.36	9.6	6.76	17.87	9.65	0.5056	23.82	9.7
2060	5.923	18.35	9.65	6.592	17.88	9.7	0.4861	23.84	9.75
2070	5.77	18.35	9.69	6.428	17.88	9.75	0.4674	23.86	9.8
2080	5.622	18.34	9.74	6.269	17.89	9.8	0.4495	23.88	9.85
2090	5.478	18.34	9.79	6.114	17.89	9.85	0.4323	23.91	9.9
2100	5.338	18.33	9.84	5.963	17.9	9.89	0.4158	23.93	9.95
2110	5.202	18.33	9.89	5.816	17.9	9.94	0.4	23.95	10.
2120	5.07	18.33	9.94	5.673	17.91	9.99	0.3848	23.98	10.05
2130	4.942	18.32	9.98	5.533	17.92	10.04	0.3702	24.	10.1
2140	4.817	18.32	10.03	5.397	17.92	10.09	0.3562	24.02	10.15
2150	4.696	18.31	10.08	5.265	17.93	10.14	0.3428	24.04	10.2
2160	4.578	18.31	10.13	5.137	17.93	10.19	0.33	24.07	10.25
2170	4.463	18.31	10.18	5.011	17.94	10.24	0.3176	24.09	10.3
2180	4.352	18.31	10.23	4.889	17.94	10.29	0.3057	24.11	10.35
2190	4.244	18.3	10.28	4.771	17.95	10.34	0.2944	24.14	10.4

Table 11. NLO contributions to the production cross-section for a scalar particle, as they are defined in eq. (5.4). The theory uncertainty is computed as in eq. (5.5).

m_S [GeV]	$\sigma_S^{\text{NLO}}[1, 1][\text{fb}]$	$\delta_{\text{th}} [\%]$	$\delta_{\alpha_S}^{\text{PDF}} [\%]$	$\sigma_S^{\text{NLO}}[1, 0][\text{fb}]$	$\delta_{\text{th}} [\%]$	$\delta_{\alpha_S}^{\text{PDF}} [\%]$	$\sigma_S^{\text{NLO}}[0, 1][\text{fb}]$	$\delta_{\text{th}} [\%]$	$\delta_{\alpha_S}^{\text{PDF}} [\%]$
2200	4.138	18.3	10.33	4.655	17.96	10.39	0.2834	24.16	10.46
2210	4.036	18.3	10.38	4.542	17.96	10.44	0.2729	24.18	10.51
2220	3.936	18.29	10.43	4.432	17.97	10.49	0.2628	24.2	10.56
2230	3.839	18.29	10.48	4.325	17.97	10.54	0.2531	24.23	10.61
2240	3.744	18.29	10.53	4.221	17.98	10.59	0.2438	24.25	10.66
2250	3.653	18.29	10.58	4.12	17.99	10.64	0.2349	24.27	10.72
2260	3.563	18.29	10.63	4.021	17.99	10.69	0.2263	24.3	10.77
2270	3.476	18.29	10.69	3.924	18.	10.74	0.218	24.32	10.82
2280	3.392	18.29	10.74	3.831	18.01	10.8	0.21	24.35	10.87
2290	3.309	18.28	10.79	3.739	18.01	10.85	0.2024	24.37	10.93
2300	3.229	18.28	10.84	3.65	18.02	10.9	0.1951	24.39	10.98
2310	3.151	18.28	10.89	3.563	18.02	10.95	0.188	24.41	11.03
2320	3.075	18.28	10.94	3.478	18.03	11.	0.1812	24.44	11.09
2330	3.001	18.28	11.	3.396	18.04	11.06	0.1747	24.46	11.14
2340	2.929	18.28	11.05	3.315	18.04	11.11	0.1684	24.48	11.19
2350	2.858	18.28	11.1	3.237	18.05	11.16	0.1624	24.51	11.25
2360	2.79	18.28	11.15	3.16	18.06	11.21	0.1566	24.53	11.3
2370	2.723	18.28	11.21	3.086	18.06	11.27	0.151	24.56	11.36
2380	2.658	18.28	11.26	3.013	18.07	11.32	0.1456	24.58	11.41
2390	2.595	18.28	11.31	2.942	18.08	11.37	0.1404	24.6	11.46
2400	2.534	18.28	11.37	2.873	18.08	11.43	0.1354	24.62	11.52
2410	2.474	18.28	11.42	2.805	18.09	11.48	0.1306	24.65	11.58
2420	2.415	18.28	11.47	2.74	18.1	11.54	0.126	24.67	11.63
2430	2.358	18.28	11.53	2.675	18.1	11.59	0.1216	24.7	11.69
2440	2.303	18.29	11.58	2.613	18.11	11.65	0.1173	24.72	11.74
2450	2.248	18.29	11.64	2.552	18.12	11.7	0.1132	24.75	11.8
2460	2.196	18.29	11.69	2.492	18.13	11.75	0.1092	24.77	11.85
2470	2.144	18.29	11.75	2.434	18.13	11.81	0.1054	24.79	11.91
2480	2.094	18.29	11.8	2.378	18.14	11.86	0.1017	24.82	11.97
2490	2.045	18.3	11.86	2.323	18.15	11.92	0.0982	24.84	12.02
2500	1.998	18.3	11.91	2.269	18.16	11.98	0.09479	24.87	12.08
2510	1.951	18.3	11.97	2.216	18.17	12.03	0.09151	24.89	12.14
2520	1.906	18.3	12.02	2.165	18.18	12.09	0.08834	24.92	12.19
2530	1.862	18.31	12.08	2.115	18.18	12.14	0.08529	24.94	12.25
2540	1.819	18.31	12.14	2.066	18.19	12.2	0.08235	24.97	12.31
2550	1.777	18.31	12.19	2.019	18.2	12.26	0.07952	24.99	12.37
2560	1.736	18.32	12.25	1.972	18.21	12.31	0.07679	25.02	12.42
2570	1.696	18.32	12.31	1.927	18.21	12.37	0.07416	25.04	12.48
2580	1.657	18.32	12.36	1.883	18.22	12.43	0.07163	25.06	12.54
2590	1.619	18.32	12.42	1.84	18.23	12.48	0.06919	25.08	12.6
2600	1.582	18.33	12.48	1.797	18.24	12.54	0.06683	25.11	12.66
2610	1.545	18.33	12.53	1.756	18.25	12.6	0.06456	25.14	12.72
2620	1.51	18.34	12.59	1.716	18.26	12.66	0.06237	25.17	12.78
2630	1.476	18.34	12.65	1.677	18.27	12.72	0.06026	25.19	12.84
2640	1.442	18.34	12.71	1.639	18.28	12.77	0.05822	25.22	12.9

Table 12. NLO contributions to the production cross-section for a scalar particle, as they are defined in eq. (5.4). The theory uncertainty is computed as in eq. (5.5).

m_S [GeV]	$\sigma_S^{\text{NLO}}[1, 1][\text{fb}]$	$\delta_{\text{th}} [\%]$	$\delta_{\alpha_S}^{\text{PDF}} [\%]$	$\sigma_S^{\text{NLO}}[1, 0][\text{fb}]$	$\delta_{\text{th}} [\%]$	$\delta_{\alpha_S}^{\text{PDF}} [\%]$	$\sigma_S^{\text{NLO}}[0, 1][\text{fb}]$	$\delta_{\text{th}} [\%]$	$\delta_{\alpha_S}^{\text{PDF}} [\%]$
2650	1.409	18.35	12.77	1.602	18.28	12.83	0.05626	25.24	12.96
2660	1.377	18.35	12.83	1.565	18.29	12.89	0.05436	25.27	13.02
2670	1.346	18.36	12.88	1.53	18.3	12.95	0.05254	25.29	13.08
2680	1.315	18.36	12.94	1.495	18.31	13.01	0.05077	25.31	13.14
2690	1.286	18.36	13.	1.461	18.32	13.07	0.04907	25.34	13.2
2700	1.257	18.37	13.06	1.428	18.33	13.13	0.04743	25.37	13.26
2710	1.228	18.38	13.12	1.396	18.34	13.19	0.04585	25.4	13.32
2720	1.201	18.38	13.18	1.364	18.34	13.25	0.04432	25.42	13.38
2730	1.174	18.38	13.24	1.333	18.35	13.31	0.04285	25.44	13.44
2740	1.147	18.39	13.3	1.303	18.37	13.37	0.04143	25.47	13.5
2750	1.121	18.4	13.36	1.274	18.37	13.43	0.04005	25.5	13.57
2760	1.096	18.4	13.42	1.245	18.39	13.49	0.03873	25.53	13.63
2770	1.072	18.41	13.48	1.217	18.39	13.55	0.03745	25.55	13.69
2780	1.048	18.42	13.54	1.19	18.4	13.61	0.03621	25.58	13.75
2790	1.024	18.42	13.61	1.163	18.41	13.68	0.03502	25.6	13.82
2800	1.001	18.43	13.67	1.137	18.42	13.74	0.03387	25.63	13.88
2810	0.9791	18.43	13.73	1.112	18.43	13.8	0.03276	25.65	13.94
2820	0.9573	18.44	13.79	1.087	18.44	13.86	0.03169	25.69	14.01
2830	0.936	18.45	13.85	1.062	18.45	13.92	0.03065	25.71	14.07
2840	0.9152	18.45	13.92	1.039	18.46	13.99	0.02965	25.74	14.13
2850	0.8949	18.46	13.98	1.016	18.47	14.05	0.02868	25.76	14.2
2860	0.8751	18.46	14.04	0.9929	18.48	14.11	0.02775	25.79	14.26
2870	0.8557	18.47	14.1	0.9708	18.49	14.17	0.02685	25.82	14.33
2880	0.8368	18.48	14.17	0.9492	18.5	14.24	0.02598	25.84	14.39
2890	0.8183	18.5	14.23	0.9281	18.51	14.3	0.02514	25.87	14.46
2900	0.8003	18.51	14.29	0.9075	18.52	14.37	0.02432	25.9	14.52
2910	0.7826	18.52	14.36	0.8874	18.53	14.43	0.02354	25.92	14.59
2920	0.7654	18.53	14.42	0.8677	18.54	14.49	0.02278	25.95	14.65
2930	0.7485	18.55	14.49	0.8485	18.55	14.56	0.02205	25.98	14.72
2940	0.7321	18.56	14.55	0.8297	18.56	14.62	0.02134	26.01	14.79
2950	0.716	18.57	14.62	0.8113	18.57	14.69	0.02065	26.03	14.85
2960	0.7003	18.59	14.68	0.7934	18.58	14.75	0.01999	26.06	14.92
2970	0.6849	18.6	14.75	0.7759	18.6	14.82	0.01935	26.09	14.99
2980	0.6699	18.61	14.81	0.7588	18.6	14.89	0.01873	26.11	15.05
2990	0.6552	18.63	14.88	0.742	18.62	14.95	0.01813	26.15	15.12
3000	0.6409	18.64	14.95	0.7257	18.63	15.02	0.01756	26.18	15.19

Table 13. NLO contributions to the production cross-section for a scalar particle, as they are defined in eq. (5.4). The theory uncertainty is computed as in eq. (5.5).

m_S [GeV]	$\sigma_S^{\text{NLO}}[1, 1][\text{fb}]$	$\delta_{\text{th}} [\%]$	$\delta_{\alpha_S}^{\text{PDF}} [\%]$	$\sigma_S^{\text{NLO}}[1, 0][\text{fb}]$	$\delta_{\text{th}} [\%]$	$\delta_{\alpha_S}^{\text{PDF}} [\%]$	$\sigma_S^{\text{NLO}}[0, 1][\text{fb}]$	$\delta_{\text{th}} [\%]$	$\delta_{\alpha_S}^{\text{PDF}} [\%]$
730	1.273	20.7	4.34	0.4417	18.35	4.38	0.5144	21.21	4.33
731	1.264	20.7	4.34	0.4398	18.34	4.39	0.5105	21.21	4.33
732	1.255	20.7	4.35	0.4379	18.34	4.39	0.5067	21.22	4.34
733	1.246	20.7	4.35	0.4359	18.34	4.39	0.5029	21.22	4.34
734	1.238	20.7	4.35	0.434	18.34	4.4	0.4991	21.22	4.34
735	1.229	20.7	4.36	0.4321	18.33	4.4	0.4953	21.22	4.35
736	1.221	20.7	4.36	0.4302	18.33	4.4	0.4916	21.23	4.35
737	1.212	20.69	4.36	0.4283	18.33	4.41	0.4879	21.23	4.35
738	1.204	20.69	4.37	0.4264	18.33	4.41	0.4843	21.23	4.36
739	1.195	20.69	4.37	0.4246	18.33	4.41	0.4806	21.23	4.36
740	1.187	20.69	4.37	0.4227	18.32	4.42	0.477	21.23	4.36
741	1.179	20.69	4.38	0.4209	18.32	4.42	0.4735	21.24	4.37
742	1.171	20.69	4.38	0.419	18.32	4.42	0.4699	21.24	4.37
743	1.163	20.69	4.38	0.4172	18.32	4.43	0.4664	21.24	4.37
744	1.155	20.69	4.39	0.4154	18.32	4.43	0.4629	21.24	4.38
745	1.147	20.69	4.39	0.4136	18.31	4.43	0.4595	21.24	4.38
746	1.139	20.69	4.4	0.4118	18.31	4.44	0.4561	21.24	4.39
747	1.131	20.69	4.4	0.41	18.31	4.44	0.4527	21.25	4.39
748	1.123	20.69	4.4	0.4082	18.31	4.44	0.4493	21.25	4.39
749	1.115	20.68	4.4	0.4064	18.31	4.45	0.446	21.25	4.4
750	1.108	20.68	4.41	0.4046	18.3	4.45	0.4427	21.25	4.4
751	1.1	20.68	4.41	0.4029	18.3	4.45	0.4394	21.25	4.4
752	1.093	20.68	4.42	0.4011	18.3	4.46	0.4361	21.26	4.41
753	1.085	20.68	4.42	0.3994	18.3	4.46	0.4329	21.26	4.41
754	1.078	20.68	4.42	0.3977	18.3	4.46	0.4297	21.26	4.41
755	1.07	20.68	4.43	0.3959	18.29	4.47	0.4265	21.26	4.42
756	1.063	20.68	4.43	0.3942	18.29	4.47	0.4233	21.26	4.42
757	1.056	20.67	4.43	0.3925	18.29	4.47	0.4202	21.26	4.42
758	1.049	20.67	4.44	0.3908	18.29	4.48	0.4171	21.26	4.43
759	1.042	20.67	4.44	0.3892	18.28	4.48	0.414	21.27	4.43
760	1.035	20.67	4.44	0.3875	18.28	4.49	0.411	21.27	4.43
761	1.028	20.67	4.45	0.3858	18.28	4.49	0.408	21.27	4.44
762	1.021	20.67	4.45	0.3842	18.28	4.49	0.405	21.27	4.44
763	1.014	20.67	4.45	0.3825	18.28	4.5	0.402	21.28	4.44
764	1.007	20.67	4.46	0.3809	18.27	4.5	0.399	21.28	4.45
765	1.	20.67	4.46	0.3792	18.27	4.5	0.3961	21.28	4.45
766	0.9934	20.67	4.46	0.3776	18.27	4.51	0.3932	21.28	4.45
767	0.9867	20.67	4.47	0.376	18.27	4.51	0.3903	21.28	4.46
768	0.9801	20.66	4.47	0.3744	18.27	4.51	0.3874	21.29	4.46
769	0.9735	20.66	4.48	0.3728	18.27	4.52	0.3846	21.29	4.46
770	0.967	20.66	4.48	0.3712	18.26	4.52	0.3818	21.29	4.47

Table 14. NLO contributions to the production cross-section for a scalar particle with a mass around 750 GeV, as they are defined in eq. (5.4). The theory uncertainty is computed as in eq. (5.5).

Open Access. This article is distributed under the terms of the Creative Commons Attribution License ([CC-BY 4.0](https://creativecommons.org/licenses/by/4.0/)), which permits any use, distribution and reproduction in any medium, provided the original author(s) and source are credited.

References

- [1] ATLAS collaboration, *Observation of a new particle in the search for the Standard Model Higgs boson with the ATLAS detector at the LHC*, *Phys. Lett. B* **716** (2012) 1 [[arXiv:1207.7214](#)] [[INSPIRE](#)].
- [2] CMS collaboration, *Observation of a new boson at a mass of 125 GeV with the CMS experiment at the LHC*, *Phys. Lett. B* **716** (2012) 30 [[arXiv:1207.7235](#)] [[INSPIRE](#)].
- [3] ATLAS collaboration, *Search for resonances decaying to photon pairs in 3.2 fb^{-1} of pp collisions at $\sqrt{s} = 13\text{ TeV}$ with the ATLAS detector*, [ATLAS-CONF-2015-081](#) (2015) [[INSPIRE](#)].
- [4] CMS collaboration, *Search for new physics in high mass diphoton events in proton-proton collisions at $\sqrt{s} = 13\text{ TeV}$* , [CMS-PAS-EXO-15-004](#) (2015) [[INSPIRE](#)].
- [5] P.A. Baikov, K.G. Chetyrkin, A.V. Smirnov, V.A. Smirnov and M. Steinhauser, *Quark and gluon form factors to three loops*, *Phys. Rev. Lett.* **102** (2009) 212002 [[arXiv:0902.3519](#)] [[INSPIRE](#)].
- [6] T. Gehrmann, E.W.N. Glover, T. Huber, N. Ikizlerli and C. Studerus, *Calculation of the quark and gluon form factors to three loops in QCD*, *JHEP* **06** (2010) 094 [[arXiv:1004.3653](#)] [[INSPIRE](#)].
- [7] M. Höschele, J. Hoff, A. Pak, M. Steinhauser and T. Ueda, *Higgs boson production at the LHC: NNLO partonic cross-sections through order ϵ and convolutions with splitting functions to $N^3\text{LO}$* , *Phys. Lett. B* **721** (2013) 244 [[arXiv:1211.6559](#)] [[INSPIRE](#)].
- [8] C. Anastasiou, S. Buehler, C. Duhr and F. Herzog, *NNLO phase space master integrals for two-to-one inclusive cross-sections in dimensional regularization*, *JHEP* **11** (2012) 062 [[arXiv:1208.3130](#)] [[INSPIRE](#)].
- [9] C. Anastasiou, C. Duhr, F. Dulat and B. Mistlberger, *Soft triple-real radiation for Higgs production at $N^3\text{LO}$* , *JHEP* **07** (2013) 003 [[arXiv:1302.4379](#)] [[INSPIRE](#)].
- [10] C. Anastasiou, C. Duhr, F. Dulat, F. Herzog and B. Mistlberger, *Real-virtual contributions to the inclusive Higgs cross-section at $N^3\text{LO}$* , *JHEP* **12** (2013) 088 [[arXiv:1311.1425](#)] [[INSPIRE](#)].
- [11] Y. Li and H.X. Zhu, *Single soft gluon emission at two loops*, *JHEP* **11** (2013) 080 [[arXiv:1309.4391](#)] [[INSPIRE](#)].
- [12] C. Anastasiou et al., *Higgs boson gluon-fusion production at threshold in $N^3\text{LO}$ QCD*, *Phys. Lett. B* **737** (2014) 325 [[arXiv:1403.4616](#)] [[INSPIRE](#)].
- [13] C. Anastasiou et al., *Higgs boson gluon-fusion production beyond threshold in $N^3\text{LO}$ QCD*, *JHEP* **03** (2015) 091 [[arXiv:1411.3584](#)] [[INSPIRE](#)].
- [14] F. Dulat and B. Mistlberger, *Real-Virtual-Virtual contributions to the inclusive Higgs cross-section at $N^3\text{LO}$* , [arXiv:1411.3586](#) [[INSPIRE](#)].

- [15] C. Duhr, T. Gehrmann and M. Jaquier, *Two-loop splitting amplitudes and the single-real contribution to inclusive Higgs production at N^3LO* , *JHEP* **02** (2015) 077 [[arXiv:1411.3587](#)] [[INSPIRE](#)].
- [16] Y. Li, A. von Manteuffel, R.M. Schabinger and H.X. Zhu, *Soft-virtual corrections to Higgs production at N^3LO* , *Phys. Rev. D* **91** (2015) 036008 [[arXiv:1412.2771](#)] [[INSPIRE](#)].
- [17] C. Anastasiou, C. Duhr, F. Dulat, F. Herzog and B. Mistlberger, *Higgs Boson Gluon-Fusion Production in QCD at Three Loops*, *Phys. Rev. Lett.* **114** (2015) 212001 [[arXiv:1503.06056](#)] [[INSPIRE](#)].
- [18] C. Anzai et al., *Exact N^3LO results for $qq' \rightarrow H + X$* , *JHEP* **07** (2015) 140 [[arXiv:1506.02674](#)] [[INSPIRE](#)].
- [19] C. Anastasiou et al., *High precision determination of the gluon fusion Higgs boson cross-section at the LHC*, *JHEP* **05** (2016) 058 [[arXiv:1602.00695](#)] [[INSPIRE](#)].
- [20] C. Anastasiou, C. Duhr, F. Dulat, E. Furlan, F. Herzog and B. Mistlberger, *Soft expansion of double-real-virtual corrections to Higgs production at N^3LO* , *JHEP* **08** (2015) 051 [[arXiv:1505.04110](#)] [[INSPIRE](#)].
- [21] HIGGS CROSS-SECTION Working Group, *BSM Higgs production cross-sections at $\sqrt{s} = 13$ TeV (update in CERN Report4 2016)*, <https://twiki.cern.ch/twiki/bin/view/LHCPhysics/CERNYellowReportPageBSMA13TeV>.
- [22] M.J. Dolan, J.L. Hewett, M. Krämer and T.G. Rizzo, *Simplified Models for Higgs Physics: Singlet Scalar and Vector-like Quark Phenomenology*, *JHEP* **07** (2016) 039 [[arXiv:1601.07208](#)] [[INSPIRE](#)].
- [23] PARTICLE DATA GROUP collaboration, S. Eidelman et al., *Review of particle physics*, *Phys. Lett. B* **592** (2004) 1 [[INSPIRE](#)].
- [24] V.P. Spiridonov and K.G. Chetyrkin, *Nonleading mass corrections and renormalization of the operators $m\psi - \bar{\psi}$ and $G_{\mu\nu}^2$* , *Sov. J. Nucl. Phys.* **47** (1988) 522 [*Yad. Fiz.* **47** (1988) 818] [[INSPIRE](#)].
- [25] K.G. Chetyrkin, B.A. Kniehl and M. Steinhauser, *Decoupling relations to $O(\alpha_S^3)$ and their connection to low-energy theorems*, *Nucl. Phys. B* **510** (1998) 61 [[hep-ph/9708255](#)] [[INSPIRE](#)].
- [26] Y. Schröder and M. Steinhauser, *Four-loop decoupling relations for the strong coupling*, *JHEP* **01** (2006) 051 [[hep-ph/0512058](#)] [[INSPIRE](#)].
- [27] J. Butterworth et al., *PDF4LHC recommendations for LHC Run II*, *J. Phys. G* **43** (2016) 023001 [[arXiv:1510.03865](#)] [[INSPIRE](#)].
- [28] S. Dulat et al., *New parton distribution functions from a global analysis of quantum chromodynamics*, *Phys. Rev. D* **93** (2016) 033006 [[arXiv:1506.07443](#)] [[INSPIRE](#)].
- [29] NNPDF collaboration, R.D. Ball et al., *Parton distributions for the LHC Run II*, *JHEP* **04** (2015) 040 [[arXiv:1410.8849](#)] [[INSPIRE](#)].
- [30] R.V. Harlander and K.J. Ozeren, *Finite top mass effects for hadronic Higgs production at next-to-next-to-leading order*, *JHEP* **11** (2009) 088 [[arXiv:0909.3420](#)] [[INSPIRE](#)].
- [31] A. Pak, M. Rogal and M. Steinhauser, *Finite top quark mass effects in NNLO Higgs boson production at LHC*, *JHEP* **02** (2010) 025 [[arXiv:0911.4662](#)] [[INSPIRE](#)].
- [32] G. Panico, L. Vecchi and A. Wulzer, *Resonant Diphoton Phenomenology Simplified*, *JHEP* **06** (2016) 184 [[arXiv:1603.04248](#)] [[INSPIRE](#)].